

# Journal Pre-Proof

Neanderthals in changing environments from MIS 5 to early MIS 4 in northern Central Europe – Integrating archaeological, (chrono)stratigraphic and paleoenvironmental evidence at the site of Lichtenberg.



**Authors:** Marcel Weiss, Michael Hein, Brigitte Urban, Mareike C. Stahlschmidt, Susann Heinrich, Yamandu H. Hilbert, Robert C. Power, Hans v. Suchodoletz, Thomas Terberger, Utz Böhner, Florian Klimscha, Stephan Veil, Klaus Breest, Johannes Schmidt, Debra Colarossi, Mario Tucci, Manfred Frechen, David C. Tanner, Tobias Lauer

**Published in:** Quaternary Science Reviews 284. 25 pages, 8 figures, 4 tables, 100 pages of supplementary information

**DOI:** 10.1016/j.quascirev.2022.107519

**Received:** 11 October 2021

**Revised:** 16 March 2022

**Accepted:** 5 April 2022

**Please cite this article as:** M. Weiss & M. Hein et al. (2022), Neanderthals in changing environments from MIS 5 to early MIS 4 in northern Central Europe – Integrating archaeological, (chrono)stratigraphic and paleoenvironmental evidence at the site of Lichtenberg, *Quaternary Science Reviews* 284. <https://doi.org/10.1016/j.quascirev.2022.107519>

1 **Neanderthals in changing environments from MIS 5 to early MIS 4 in northern Central**  
2 **Europe – Integrating archaeological, (chrono)stratigraphic and paleoenvironmental**  
3 **evidence at the site of Lichtenberg**

4  
5 Marcel Weiss\*<sup>1,2</sup>, Michael Hein\*<sup>1</sup>, Brigitte Urban<sup>3</sup>, Mareike C. Stahlschmidt<sup>1</sup>, Susann  
6 Heinrich<sup>1</sup>, Yamandu H. Hilbert<sup>2</sup>, Robert C. Power<sup>4,1</sup>, Hans v. Suchodoletz<sup>5</sup>, Thomas  
7 Terberger<sup>6</sup>, Utz Böhner<sup>6</sup>, Florian Klimscha<sup>7</sup>, Stephan Veil<sup>7</sup>, Klaus Breest<sup>8</sup>, Johannes Schmidt<sup>5</sup>,  
8 Debra Colarossi<sup>9,1</sup>, Mario Tucci<sup>3</sup>, Manfred Frechen<sup>10</sup>, David Colin Tanner<sup>10</sup> & Tobias Lauer<sup>1</sup>  
9

10 <sup>1</sup>Max Planck Institute for Evolutionary Anthropology, Leipzig, Germany

11  
12 <sup>2</sup>Institut für Ur- und Frühgeschichte, Friedrich-Alexander-Universität Erlangen-Nürnberg,  
13 Erlangen, Germany

14  
15 <sup>3</sup>Leuphana University Lüneburg, Institute of Ecology, Lüneburg, Germany

16  
17 <sup>4</sup>Institute for Pre- and Protohistoric Archaeology and Archaeology of the Roman Provinces,  
18 Ludwig Maximilian University Munich, Germany

19  
20 <sup>5</sup>Institute of Geography, Leipzig University, Leipzig, Germany

21  
22 <sup>6</sup>State Service for Cultural Heritage Lower Saxony, Hannover, Germany

23  
24 <sup>7</sup>Lower Saxony State Museum, Department for Research and Collections, Archaeology  
25 Division, Hannover, Germany

26  
27 <sup>8</sup>Volunteer archaeologist, Berlin, Germany

28  
29 <sup>9</sup>Department of Geography and Earth Sciences, Aberystwyth University, Aberystwyth, Wales,  
30 UK

31  
32 <sup>10</sup>Leibniz Institute for Applied Geophysics, Stilleweg 2, Hannover, Germany

33  
34 \*Equal contributions.

35  
36 **Keywords**

37 Middle Paleolithic, Neanderthals, Quaternary stratigraphy, luminescence dating, palynology

38  
39 **Abstract**

40 The resilience of Neanderthals towards changing climatic and environmental conditions, and  
41 especially towards severely cold climates in northern regions of central Europe, is still under  
42 debate. One way to address this is to investigate multi-layered occupation in different climatic  
43 intervals, using independently-compiled paleoenvironmental and chronological data.  
44 Unfortunately, most open-air sites on the northern European Plain lack a robust  
45 chronostratigraphy beyond the radiocarbon dating range, thereby often hampering direct

46 links between human occupation and climate. Here we present the results of integrative  
47 research at the Middle Paleolithic open-air site of Lichtenberg, Northern Germany, comprising  
48 archaeology, luminescence dating, sedimentology, micromorphology, as well as pollen and  
49 phytolith analyses. Our findings clearly show Neanderthal presence in temperate, forested  
50 environments during the Mid-Eemian Interglacial, MIS 5e and the latest Brörup Interstadial,  
51 MIS 5c/GI 22 (Lichtenberg II). For the previously known occupation Lichtenberg I, we revise  
52 the chronology from the former early MIS 3 ( $57 \pm 6$  ka) to early MIS 4/GS 19 ( $71.3 \pm 7.3$  ka),  
53 with dominant cold steppe/tundra vegetation. The early MIS 4 occupation suggests that  
54 Neanderthals could adjust well to severely cold environments and implies recurring  
55 population in the region between MIS 5 and MIS 3. The artefact assemblages differ between  
56 the temperate and cold environment occupations regarding size, blank production, typology  
57 and tool use. We argue that this distinctness can partially be explained by different site  
58 functions and occupation duration, as well as the availability of large and high-quality flint raw  
59 material. Raw material availability is in turn governed by changing vegetation cover that  
60 hindered or fostered sediment redeposition as a provider of flint from the primary source of  
61 the glacial sediments nearby.

62

### 63 **1. Introduction**

64 The “stereotype” Neanderthal is mostly perceived as a human species that lived in the cold  
65 and harsh climatic environments of the past glacial periods in Eurasia. But were Neanderthals  
66 indeed adapted to cold environments? This question has been a matter of debate in  
67 prehistory, biology and physical anthropology for a long time (e.g., Aiello and Wheeler, 2003;  
68 Churchill, 2008; Rae et al., 2011; Skrzypek et al., 2011; White and Pettitt, 2011). One way of  
69 addressing this open question is to analyze Neanderthal occupation at the northern extreme  
70 of their habitat, more precisely the northern part of Central Europe.

71 Currently, numerous sites suggest that Neanderthals settled in northern Central Europe  
72 during the Eemian Interglacial and during the first half of the last glacial cycle (Gaudzinski-  
73 Windheuser and Roebroeks, 2014; Hein et al., 2020; Litt and Weber, 1988; Nielsen et al., 2017;  
74 Richter, 2016; Thieme and Veil, 1985; Toepfer, 1958; Weber, 1990). However, the chronology  
75 of most late Middle Paleolithic sites is either poor and/or controversial (Jöris, 2004; Mania,  
76 2002; Pastoors, 2009, 2001; Veil et al., 1994), and many of them are not dated at all. The  
77 majority of those sites are classified as late Middle Paleolithic by typological means only

78 (Kegler and Fries, 2018; Richter, 2016). Due to this lack of precise site chronologies, even  
79 though we know that Neanderthals occupied the northern regions, we lack evidence of  
80 whether they stayed there only during warmer periods of the last interglacial - glacial cycle or  
81 if they also persisted through cold stadial conditions. So far, the only indication for the latter  
82 is the site of Salzgitter-Lebenstedt, Lower Saxony/ Germany (Tode, 1982). At this site, the finds  
83 originate from layers containing cold climatic vegetation remains (Pastoors, 2001;  
84 Pfaffenberg, 1991; Selle, 1991), and are associated with glacial fauna. The presence of cranial  
85 and post-cranial Neanderthal remains (Hublin, 1984), clearly link Neanderthals to the  
86 accumulation of archaeological and faunal remains at the site. They hunted reindeer and  
87 manufactured bone tools from mammoth ribs (Gaudzinski, 1999, 1998). However, the dating  
88 of the site still lacks resolution. Uncertain ages at the upper limit of the <sup>14</sup>C time scale, together  
89 with contrasting stratigraphic interpretation, place the site either in the Marine Isotope Stage  
90 (MIS) 5a/4 (Jöris, 2004) or MIS 4/3 transition (Pastoors, 2009, 2001). Furthermore, the  
91 integrity of the lithic assemblage is unclear, as the artefacts were found in several geological  
92 layers (Pastoors, 2001). Evidence for occupation during warmer early last glacial interstadials  
93 only comes from two sites of the northern Central European Plain so far. The first site is  
94 Neumark-Nord 2/0 (Laurat and Brühl, 2006), Saxony-Anhalt/ Germany dating to either MIS 5c  
95 or 5a (Richter and Krbetschek, 2014; Strahl et al., 2010). The second site is Königsau (Mania  
96 and Toepfer, 1973), Saxony-Anhalt/ Germany. Neanderthal occupation is here associated with  
97 peat layers at a paleo-lakeshore, dating most probably to MIS 5a (Jöris, 2004; Mania, 2002;  
98 Mania and Toepfer, 1973; but see Hedges et al., 1998 for a potential MIS 3 age of the site).  
99 However, with the scarce evidence outlined above, it is currently not possible to reconstruct  
100 the timing of human presence in northern Central Europe, as well as behavioral response to  
101 short-term climatic shifts.

102 To address these issues, we need to contextualize the northern Neanderthal occupations  
103 using detailed paleoenvironmental reconstructions, derived from the same  
104 chronostratigraphic frameworks as the archaeological material, preferably with a temporal  
105 resolution on the millennial scale of Greenland Interstadials (Rasmussen et al., 2014). Since  
106 the Middle Paleolithic period is mostly outside the radiocarbon range, this kind of precision is  
107 usually reserved for loess regions, where highly-resolved sediment-paleosol sequences occur  
108 (Locht et al., 2016). Beyond the loess belt, at the northern margin of the Neanderthal habitat  
109 and the European Plain, occupation is conceived to have been most particularly affected by

110 climatic fluctuations (Depaepe et al., 2015; Hublin and Roebroeks, 2009; Roebroeks et al.,  
111 2011). Across these landscapes, however, shallow sediment deposits in unison with frequent  
112 cryoturbation features often hamper the establishment of such a precise chronostratigraphic  
113 framework (Hein et al., 2020; Wiśniewski et al., 2019). Instead, the dating resolution  
114 commonly does not exceed the much coarser scale of Marine Isotope Stages (Lisiecki and  
115 Raymo, 2005a).

116

117 Here we present new results of our recent research at the late Middle Paleolithic open-air site  
118 complex of Lichtenberg, Lower Saxony/Germany (Veil et al., 1994), which was initially  
119 discovered in 1987 and excavated until 1993 by the Niedersächsisches Landesmuseum,  
120 Hannover, Germany. Lichtenberg represents a Neanderthal site at the potential northern limit  
121 of their geographic range (Nielsen et al., 2017). The site yielded one of the most prominent  
122 late Middle Paleolithic assemblages of the northern Central European Plain, as well as a  
123 sediment sequence encompassing deposits from MIS 5e through MIS 3 (Veil et al., 1994).  
124 Neanderthal occupations at Lichtenberg were associated with a paleo-lakeshore (Hein et al.,  
125 2021). Therefore, the long-lasting highly resolved sediment sequence composed of  
126 intercalated organic and clastic sediments is an ideal location to study climatic and  
127 environmental shifts, and to investigate the Neanderthal population dynamics at the northern  
128 limit of their habitat.

129 Our multidisciplinary investigations combine archaeological investigations with detailed  
130 sedimentological, chronological and paleoenvironmental studies of the find-bearing and  
131 associated non-find bearing layers of the sequence. Our research focusses on the following  
132 aims: (1) Can we connect Neanderthal occupations of northern Central Europe to a  
133 chronological resolution of Greenland Interstadial-Stadial level and thus to changing climatic  
134 conditions? (2) Did Neanderthals inhabit specific environments only, or did they adapt to  
135 different environmental conditions? (3) To which extent do archaeological assemblages vary  
136 in different environments and climates? And, most importantly, (4) did Neanderthals live in  
137 northern Central Europe only during warmer, forested phases of the last glacial, or could they  
138 also cope with cold climatic conditions and open landscapes in the stadials of the Early  
139 Weichselian and the Pleniglacial?

140

141

142 **2. Materials**

143 **2.1 Study area**

144 Based on archaeological evidence and (paleo-)geographical considerations, the study region,  
145 here referred to as “northern Central Europe” or “northern Central European Plain”, consists  
146 mainly of the Northern German Lowlands above approximately 51° N, as well as the northern  
147 Netherlands. Today, the latter is part of the rather maritime North-Western Europe, but due  
148 to the lower sea level during the last glacial cycle, the northern Netherlands were part of a  
149 more extensive northern Central European Plain, and thus incorporated into the study region.  
150 Northern Poland is not included here, as we currently lack Middle Paleolithic archaeological  
151 sites from the area covered by the ice shield of the last Glaciation (see e.g., Wiśniewski et al.,  
152 2013).

153

154 **2.2 Geological setting**

155 The study site is located at latitude 52°55' N in Northern Germany, eastern Lower Saxony (Fig.  
156 1a). Throughout the Pleistocene, Scandinavian glaciers covered the region twice during the  
157 Elsterian (MIS 12) and three times during the Saalian (MIS 6) glaciation, and deposited >40 m  
158 of glacial tills and glaciofluvial sands (Ehlers et al., 2011; Lang et al., 2018). The ice-marginal  
159 valley of the River Elbe, as the major drainage channel of the region, assumed its course close  
160 to the study area, already during the late Saalian Warthe Stadial (Fig. 1) (Ehlers, 1990; Meyer,  
161 1983). In contrast, Weichselian glaciers during MIS 4 and MIS 2 did not cross the Elbe  
162 lineament, with the margin of the furthest advance situated ca. 50 km to the NE (Duphorn et  
163 al., 1973; Ehlers, 2020) of the study area. The archaeological site is located at the southern  
164 declivity of the Öring, a confined Saalian plateau, which passes over into a major sediment  
165 basin that repeatedly hosted a lakescape since at least the Saalian-Eemian transition (Hein et  
166 al., 2021). Therefore, in the course of the Weichselian, the depositional regime was mainly  
167 characterized by slopewash and periglacial processes (Veil et al., 1994), which were  
168 presumably interrupted by episodic lake transgressions (Hein et al., 2021).

169 Neanderthal occupation took place on a small alluvial fan, which likely formed between the  
170 late Eemian Interstadial and early Weichselian Pleniglacial and provided a higher and hence  
171 drier ground, in comparison to the surrounding wetlands (ibid., Fig. 1b, Supplementary Figure  
172 S49b).

173

## 174 **2.3 Previous Investigations**

### 175 **Archaeological Horizon Lichtenberg I**

176 The site Lichtenberg with its archaeological horizon Lichtenberg I (hereafter: Li-I) was  
177 discovered in 1987 by one of us (K.B.) and was subsequently excavated from 1987 to 1993  
178 (Veil, 1995; Veil et al., 1994). The assemblage consists of about 2500 artefacts, among them  
179 405 artefacts with recorded provenience, including 76 retouched tools (Veil et al., 1994). All  
180 artefacts are made of Baltic Flint. Most of the bifacial tools were manufactured on natural  
181 blanks, such as frost shards transported from the Saalian glacial deposits upslope and  
182 potentially directly available on the land surface (Veil et al., 1994). Cores are entirely missing  
183 in the assemblage, but faceted flake platforms may hint at the existence of Levallois blank  
184 production (Veil et al., 1994). However, faceting may rather be the result of bifacial tool  
185 production (Veil et al., 1994; Wiśniewski et al., 2020) in this assemblage. Among the 76 tools  
186 are 19 bifacial backed knives or Keilmesser, 5 handaxes, as well as other types of bifacial tools.  
187 Keilmesser are asymmetric, mostly bifacial cutting tools with a natural and/or worked back  
188 opposite a working edge (Bosinski, 1967; Jöris, 2012, 2006; Veil et al., 1994). All of the tools  
189 have been interpreted as functionally slightly different cutting tools (Veil et al., 1994; Weiss,  
190 2020). With a median dimension (largest width or length) of 86 mm (Supplementary Table S7)  
191 for 19 bifacial and 3 unifacial Keilmesser and one handaxe (Weiss, 2020), the tools are quite  
192 large. The assemblage is attributed to the late Middle Paleolithic Keilmessergruppen of central  
193 and eastern central Europe (Jöris, 2012, 2006; Mania, 1990; Veil et al., 1994). This represents  
194 a late Neanderthal archaeostratigraphic unit that ranges from MIS 5a to early MIS 3 (Hein et  
195 al., 2020; Jöris, 2006, 2004), and which is defined by the presence of Keilmesser. Furthermore,  
196 these assemblages are characterized by handaxes and other bifacial tools (Bosinski, 1967; Veil  
197 et al., 1994), as well as by varying blank production methods, including Levallois (Jöris, 2004;  
198 Richter, 1997). Most of the Keilmesser found in Lichtenberg I are still suitable for cutting with  
199 angles below 60° (Gladilin, 1976; Weiss, 2020), and several refits (Veil et al., 1994) evidence  
200 the production and use of the tools on the spot. This, as well as the functional uniformity point  
201 to a specialized assemblage that was produced during a short-term event, and potentially  
202 related to butchering activities, as indicated by use-wear analyses (Veil et al., 1994). The  
203 formerly-obtained thermoluminescence ages for the sediments containing the artefacts range  
204 from 66±14.6 ka to 52±6.8ka (Veil et al., 1994), displaying a rather high dating uncertainty  
205 most likely resulting from the cryoturbated context in which they were found.

206

### 207 ***Evidence for Eemian occupation***

208 During our coring campaign, recently published in Hein et al. (Hein et al., 2021), we recovered  
209 a longitudinal broken flint flake (LIA-86, Supplementary Figure S13), another flint flake (LIA-  
210 187, Supplementary Figure S13), as well as a number of undetermined small chips and  
211 fragments from sandy Eemian half bog deposits of core PD.030 (6 m depth) (Fig.1c). Some of  
212 the flint fragments are highly weathered due to the acidic, humic sedimentary environment.  
213 The two artefacts are referred to as Lichtenberg Eemian and can be attributed to Eemian  
214 pollen zone E IVb/V (Hein et al., 2021). These finds make this the northernmost Eemian site  
215 besides Lehringen, Lower Saxony/ Germany (Hein et al., 2021; Nielsen et al., 2017; Thieme  
216 and Veil, 1985).

217

## 218 **3. Methods**

### 219 **3.1 Fieldwork**

220 In 2017, we localized the exact position of the 1987-1993 excavation and conducted a first  
221 attempt to locate non-cryoturbated sediments below the former trench. Then in 2019, we  
222 established geoarchaeological survey Trench 1 with a size of ca. 3 by 20 m and a depth of  
223 2.20 m (Fig. 1c, Fig. 2a; Supplementary Figures S2 – S3). In order to better understand the  
224 stratigraphical situation of Li-I, we deliberately established Trench 1 at the southern edge of  
225 the former excavation area. Here, increasing accommodation space towards the adjacent  
226 sedimentary basin suggested less cryoturbational disturbance of the deposits. From there on,  
227 Trench 1 was extended 7 m to the south, and then, to gain a W-E profile, 7.50 m to the east  
228 and another 6 m to the south. The trench was excavated by a mechanical digger and every  
229 digger bucket was carefully searched for artefacts. If artefacts were found, the respective  
230 square meter was excavated following current standards of paleolithic excavation. We  
231 excavated the sediment by hand according to individual layers, recorded all individual finds  
232 with a total station at a size cut-off of 1.5 cm and screened the excavated sediment with a  
233 4 mm and a 2 mm mesh.

234 Furthermore, we established a north-south trending coring transect of 11 sediment cores with  
235 depths of up to 11 m. The transect started upslope, and passed through the excavation area  
236 towards the valley bottom (Hein et al., 2021). The aim was to obtain high-resolution  
237 sedimentological data about the paleolake infill. Approximately 25 m north of Trench 1, at a

238 depth of ca. 2 m, we detected lakeshore sediments. Therefore, in this area, we established  
239 the second survey Trench 2 (Figs. 1c, 2b/c; Supplementary Figure S8), using the same  
240 geoarchaeological survey methods as described above. At the end of the field campaign 2019,  
241 we detected the Lichtenberg II (Li-II) find horizon in sandy and peaty lakeshore sediments and  
242 excavated one square meter before the season ended.

243 In March and June 2020, we continued fieldwork and excavated parts of the new find horizon,  
244 Li-II. The find horizon was located about 30 cm above the ground water table, necessitating  
245 the installment of a protection and water management system (Supplementary Figure S9).

246 All three stratigraphies presented here (Trenches 1 and 2, core PD.028, Figs. 1c, 2) were  
247 carefully described in the field, according to German soil mapping standards (AGBoden, 2005).

248 Documented parameters included textural composition, structure, Munsell color, carbonate  
249 and gravel content, as well as hydromorphic properties. Moreover, we documented sediment  
250 structures such as bedding and cryogenic features. This allowed for the comparison and  
251 correlation of sediment units between the stratigraphies, and facilitated optimal sampling and  
252 interpretation of luminescence samples. Further stratigraphic and landscape context was  
253 provided by the remaining cores of the more extensive drilling campaign in the study area  
254 (Hein et al., 2021).

255 3D models and Augmented Reality 3D models of both trenches can be found under  
256 <https://marcelweiss.github.io/Lichtenberg/>.

257

### 258 **3.2 Luminescence dating**

259 In total, 11 samples were taken for luminescence dating, utilizing stainless steel tubes.  
260 Sampling positions are indicated in Fig. 2a/b. The material was prepared under subdued light  
261 conditions with standard methods (Aitken, 1998). As the quartz grains showed signs of early  
262 saturation (occasionally at 80 to 100 Gy) and inconsistent dose recovery, all measurements  
263 were conducted on coarse grain K-feldspars (125-180  $\mu\text{m}$ ) using a Risø TL-DA-20 reader,  
264 equipped with IR light-emitting diodes, transmitting at 870 nm. The signal was filtered through  
265 a D-410 Chroma filter to allow detection in the blue-violet wavelength range. For sample  
266 irradiation, a calibrated  $^{90}\text{Sr}/^{90}\text{Y}$  beta source was used with a dose rate of about 0.2 Gy/s. For  
267 each sample, we prepared 24 discs with very small aliquot sizes (0.5 mm) to perform multiple  
268 grain measurements applying the pIRIR<sub>290</sub> SAR protocol (Thiel et al., 2011) and using an  $a$ -  
269 value of  $0.11 \pm 0.02$  (Kreutzer et al., 2014). Aliquots with a recycling ratio >10 % and a

270 recuperation >5 % were excluded from age calculations. Dose rates were determined by high-  
271 resolution germanium gamma spectrometry in the VTKA laboratory Dresden (Supplementary  
272 Table S13). Further information on quality assessment and the results of dose rate  
273 determinations may be found in the Supplementary Section 6.

274

### 275 **3.3 Palynological analysis**

276 For biostratigraphic control and to obtain further paleoenvironmental information, we  
277 performed palynological analysis on 12 selected samples (see Fig. 2b/c, Tab. 1 and  
278 Supplementary Figure S59 for sampling positions and lithological descriptions). From Trench  
279 2, a sequence of four samples from the peaty detrital mud (samples 4 to 7; layer 11b) and  
280 supplementing bulk samples (samples 1 to 3, 8) from layers 11 (a/b/b<sub>2</sub>) and 10 were taken.  
281 Layers 9 and 7 in Trench 1 were also sampled, but contained no pollen. Additionally, four  
282 samples (9 to 12) were retrieved from organogenic segments of the adjacent sediment core  
283 PD.028 (Supplementary Figure S59). All samples were treated with standard methods (Faegri  
284 et al., 1989; Moore et al., 1991), after which, pollen and spores were identified using the  
285 atlases of Faegri et al. (1989), Moore et al. (1991) and Beug (2004). Micro-charcoal particles  
286 < 100 µm were counted in samples 1 to 8 and are presented alongside the pollen diagrams  
287 (Supplementary Figures. S 60 and 61). The pollen sum, on which percentages of all taxa are  
288 based, is solely composed of terrestrial taxa, excluding cryptogams, Ericaceae, Cyperaceae and  
289 aquatic plants. The curve “Ericaceae indeterminate” characterizes badly preserved and  
290 therefore indeterminable Ericaceae tetrads. The arboreal pollen (AP) sum includes trees and  
291 shrubs, whereas the non-arboreal pollen (NAP) sum covers Poaceae, *Cerealia*-type and the  
292 group of terrestrial herbs. Pollen percentages and concentrations were calculated and  
293 displayed with the software package TILIA (Grimm, 1990). For detailed results and  
294 interpretation, see section 4.3 and Supplementary Section 7.

295

### 296 **3.4 Phytolith analysis**

297 To complement the palynological findings, we vertically sampled sediment from Trench 1,  
298 layer 7 (one sample each from the eastern and southern profile: samples MH1 and MH3), layer  
299 8 (MH4) and layer 9 (MH5), and also from layer 11a in Trench 2 (sample MH2)(Fig. 2,  
300 Supplementary Table S15). Phytoliths were extracted from the sediment using a version of the  
301 Rapid Phytolith Extraction method at the Max Planck Institute for Evolutionary Anthropology

302 (Katz et al., 2010). Phytoliths were counted on single and multi-cell counts using standard  
303 methods (Power et al., 2014). We aimed to count >200 phytoliths per sample but in some  
304 phytolith-poor samples, we could only reach 150-200. Phytolith concentrations based on the  
305 acid insoluble fraction (AIF) were also calculated to assess sediment diagenesis. Detailed  
306 sample preparation, results and interpretation can be found in Supplementary Section 8.

307

### 308 **3.5 Micromorphology**

309 We collected five oriented block samples for micromorphological analysis. Samples LIB 19 1  
310 and LIB 19 2 were taken from Trench 1, samples LIB 19 3 to LIB 19 5 from Trench 2 (Fig. 2d,  
311 Supplementary Figure S50). Thin sections were prepared by G. MacLeod (University of Stirling,  
312 UK) and their analysis was performed on a petrographic microscope with a magnification of  
313 20x to 200x using oblique incident (OIL), plane- (PPL) and cross-polarized light (XPL).  
314 Micromorphological descriptions follow established nomenclatures (Stoops, 2003; Stoops et  
315 al., 2010). Results and interpretation can be found in section 4.4 of the main text and in the  
316 Supplementary Section 5.3.

317

### 318 **3.6 Grain size analysis**

319 To support field descriptions and for the better assessment of sedimentary environments, we  
320 conducted grain size analysis on 28 bulk samples from most layers in both trenches (all except  
321 1, 2, 8 and 11b) at the Leibnitz Institute for Applied Geophysics, Hannover/ Germany (see Tab.  
322 1 for lab codes and positions). We utilized a Beckman-Coulter LS 13320 PIDS laser  
323 diffractometer, which detects a spectrum from 0.04 to 2000 µm. We mostly followed the  
324 measurement protocol described by Machalett et al. (2008). Deviating from this, for  
325 dispersion, we treated the samples with 1 % ammonium hydroxide solution (NH<sub>4</sub>OH) and  
326 planted them in overhead rotators for > 12 hours. We refrained from removing organic matter  
327 and carbonates as pre-tests implied low contents, which were shown to be negligible for the  
328 grain size distribution (Beuselinck et al., 1998). All samples were subjected to a fivefold  
329 measurement and subsequently averaged, whereby sample clusters with a standard deviation  
330 >5 % were rejected.

331

332

333

334 **3.7 Lithic analysis**

335 The lithic artefacts were recorded using a detailed attribute recording system, published in  
336 detail recently (Weiss, 2019, 2015). For the aim of this study, mainly the following attributes  
337 were selected from the dataset (see Supplementary Sections 3.5 – 3.7): the raw material, the  
338 state of preservation, the blank type, maximum length, width, thickness, and weight. Here,  
339 the maximum dimensions were measured, whereby flake length was measured in flaking  
340 direction. The length of cores was measured in the direction of the last flake removal. The  
341 maximum length of flake tools was also measured in flaking direction, whereas the length of  
342 tools made from cores or natural blanks was measured along the technical axis (i.e., in  
343 direction of the longest working edge). Furthermore, for the flakes were recorded: the state  
344 of the platform, the exterior platform angle (EPA), the amount of worked surface on the dorsal  
345 face (i.e., flake scars), and the direction of the dorsal scars. For cores, the amount of worked  
346 (flaked) surface was recorded, as well as the number of flaking surfaces, the number of flake  
347 scars, the flaking (or striking) angle, the condition of the striking surface, and the flaking  
348 directions. Because the tools from Li-II are typologically diverse, and often combine several  
349 types on single tools together with recycling and reuse (see below), we could not always apply  
350 strict typological schemes. Where possible (e.g., notches, denticulates), types from the  
351 Bordian typology were adopted (Bordes, 1961; see also Pop, 2014 for the use of types in  
352 Eemian assemblages). Besides retouched flakes, flakes with possible macroscopic use-wear  
353 were also counted as flake tools.

354 The full attribute dataset is available as Supplementary Datafile (.csv).

355

356 **3.8 Traceology**

357 To provide additional data on the nature of the Neanderthal occupation at the Middle  
358 Paleolithic sites of Lichtenberg I and II, traceological analysis were conducted on a sample of  
359 27 artefacts. Traceology (Semenov, 1964) aims to identify specific taphonomical, technological  
360 and functional traces or modifications, which allows us to reconstruct (i) specific technical  
361 behaviors, (ii) the post-depositional history of anthropic inclusions within sedimentary units,  
362 as well as (iii) how and for which purpose stone tools were made and used at a specific site.  
363 This is achieved by systematically scanning the edges and surfaces of stone tools under  
364 different magnifications ranging between 0.63x to 500x and plotting their location and  
365 distribution. The location and morphology of specific micro negatives, edge rounding,

366 microscopic polish, micro scars and striations are compared to an experimental reference  
367 collection in order to establish the kinetics of stone tool use as well as the worked material  
368 (Chan et al., 2020; González-Urquijo and Ibañez-Estéves, 1994; Keeley, 1980; Vaughan, 1985).  
369 Here, we used a Carl Zeiss Stemi 508 stereo microscope and an Olympus BXFM reflected light  
370 microscope.

371

## 372 **4. Results**

### 373 **4.1 Stratigraphy**

#### 374 **General Stratigraphy**

375 The sedimentary record within the Trenches 1 and 2 can be subdivided into 11 sediment layers  
376 (Fig. 2, Tab 1). The majority of these sediments are the product of the redeposition of Saalian  
377 glaciofluvial sands on the slope by different processes and over short distances (<100 m).  
378 These processes include solifluctive, niveofluvial, aeolian deposition. Furthermore, lacustrine  
379 deposits occur (see more detailed information in Supplementary Sections 5.1 and 5.2):

380 *Solifluctive deposits* (layers 2 and 3): Deposition and redeposition of solifluctive sediments  
381 happens in periglacial environments under the influence of seasonally thawing permafrost  
382 (French, 2008). This usually leads to unbedded sediments. However, as solifluction can  
383 alternate with slopewash or aeolian sedimentation, internal stratification of respective layers  
384 may occur, as is the case in layer 3.

385 *Niveofluvial deposits* (layers 4, 8 and 9): Niveofluvial deposition is a slopewash triggered by  
386 annual snowmelt in sparsely-vegetated environments together with possible involvement of  
387 aeolian input (Christiansen, 1998a; Menke, 1976; Zagwijn and Paepe, 1968). This results in the  
388 formation of thin wavy beds of fine and middle sands, and sometimes gravel.

389 *Aeolian deposits* (layer 5): Evidence for purely aeolian sedimentation of layer 5 is provided by  
390 its mean grain size (ca. 350  $\mu\text{m}$ ), good sorting and inclined bedding (ca. 15°), in combination  
391 with abundant surficial impact scars and a notably loose overall structure. There are  
392 indications that this aeolian material has been transported by saltation rather than in  
393 suspension (cf. Farrell et al., 2012; Schwan, 1988) (see Supplementary Sections 5.1 and 5.2).

394 *Lacustrine deposits* (layers 7, 10 and 11): In contrast to these slope and sensu stricto periglacial  
395 deposits from proximal sources, these layers are of lacustrine origin, i.e. their formation is  
396 connected to the presence of a paleolake (see directly below and Supplementary Sections 5.1  
397 and 5.2).

398

399 Eight of the eleven layers were encountered in both trenches. Correlation was based on the  
400 agreement of macroscopic properties detected during field work, as well as  
401 micromorphological evidence and detailed evaluation of the grain size data (Figs 2 and 3,  
402 Supplementary Sections 5.2 and 5.3). The upper part of the sequence was subjected to likely  
403 multi-phased cryoturbation in the form of different involutions, both directed upwards and  
404 downwards (Fig. 2). With amplitudes of several decimeters to nearly one meter, these  
405 phenomena were likely produced by permafrost dynamics (cf. Vandenberghe, 2013). These  
406 features are frequent in layers 1 to 6, occasionally reaching down to layer 9, and result in a  
407 somewhat fragmentary appearance of archaeological find horizon Li-I (stratigraphic layers 7  
408 and 8). Nevertheless, based on field observations, Li-I can predominantly be identified in an  
409 in-situ stratification. Find horizon Li-II in stratigraphic layer 11 remained entirely unaffected  
410 by those involutions.

411 Based on the lithological findings in Trenches 1 and 2, a schematic stratigraphy was  
412 established (see sections 5.2 and 5.3, Fig. 7), which in turn can be largely correlated with the  
413 sediment sequence of core PD.028, directly adjoining Trench 1 to the south (Figs. 1, 2;  
414 Supplementary Figure S59). The core penetrated most layers encountered in the excavations.  
415 In addition, it exposes three organogenic segments within and below niveofluvial sands,  
416 equivalent to layer 9: A peaty mud (230-250 cm coring depth) and a strongly humiferous sand  
417 (355-390 cm coring depth) surrounded by these niveofluvial sands, and a peaty layer (465-555  
418 cm coring depth) directly at their base. These organic-rich deposits testify to the wetlands that  
419 surrounded the former occupation site on an alluvial fan (Fig. 1, Supplementary Figure S49b)  
420 (description of core PD.028 in Supplementary Table S11).

421

#### 422 **Stratigraphy of the find layers Li-II and Li-I**

423 Because of their archaeological significance, the occupational layers deserve closer  
424 consideration. Layer 11, only present in Trench 2 is a two-part formation (11a and 11b), whose  
425 members interfinger with each other (Fig. 2c). Layer 11a (Li-II) is a slightly humic, unstratified  
426 silty fine sand, containing horizontally-oriented fragments of (charred) plant material and  
427 several thin humic drift lines, that are visible both macro- and microscopically (Supplementary  
428 Figures S52c, S59). We interpret this deposit as the beach facies of an adjoining water body  
429 (cf. Bridge and Demicco, 2008; Cohen, 2003), with the drift lines indicating fluctuations in the

430 water-table. Layer 11b is a peaty and sandy, coarse-detrital mud with a thickness of ca. 10 cm.  
431 It grades into a humic silt (11b2) to the top and towards the intersection with layer 11a  
432 (Supplementary Figure S59). Layer 10 is a thin (<10 cm) veneer of laminated, fine-sandy, loamy  
433 silt, that covers layer 11a. It also contains a humic drift line, and it directly emerges from the  
434 peaty detrital mud (layer 11b) and wedges out on higher ground. This layer 10 is interpreted  
435 as a lacustrine muddy shore-face deposit, caused by a rising water table (see Supplementary  
436 Section 5.1). The artefacts are scattered between a total elevation of Z=18.84 m and Z=19.55  
437 m [a.s.l.] within layer 11a. This scattering is mainly caused by the inclination of the find layer  
438 towards the shore. However, based on the distribution of screen finds < 1.5 cm within each  
439 quarter square, as well as the exact position of single finds > 1.49 cm, we could identify a main  
440 artefact scatter in the uppermost part of layer 11a, between Z = 19.10 m and Z = 19.21 m  
441 (Supplementary Section 2.2). This distribution pattern reduces the thickness of the main find  
442 horizon to 11 cm. In addition, some artefacts were obtained from the contact zone of the top  
443 part of layer 11a and the bottom part of layer 11b (as 11b interfingers with 11a).

444 Find horizon Li-I (primarily in Trench 1) is mainly contained within stratigraphic layer 7 but also  
445 includes the upper part of layer 8 (Fig. 2a). It is possible that we have evidence here for  
446 succeeding occupations, which needs to be clarified by future field work. Layer 8 is a massive  
447 to crudely-bedded, niveofluvial slopewash deposit, consisting of gravelly medium sands with  
448 gleyic properties. The layer is discordantly overlain by layer 7, a thin (<10 cm) whitish, very  
449 fine-sandy silt to silty very fine sand. Our layer 7 matches the sedimentological characteristics  
450 of the main Middle Paleolithic find horizon as described in Veil et al. (1994). In the thin  
451 sections, layer 7 stands out for its remarkably low porosity and fine horizontal layering.  
452 Because of these properties comparable with layer 10, we likewise interpret layer 7 as  
453 lacustrine shoreface deposit. In Trench 2, layer 7 intertongues with the underlying slope  
454 deposits of layer 9. The single tongues of interbedded lacustrine sediments from layer 7 unify  
455 on top of layer 9 towards higher ground (Fig 2c). This indicates alternating conditions of slope  
456 and lacustrine deposition, and testifies to their broad contemporaneity. Due to cryoturbation,  
457 layer 7 with the contained artefacts is occasionally deformed upwards in the form of diapirs  
458 or injections (then referred to as layer 7'). Based on the small number of artefacts recovered  
459 during our fieldwork (see below), we were not able to perform a statistical find distribution  
460 analysis for Li-I in our excavation. In this regard, the reader is referred to Veil et al. (Veil et al.,  
461 1994).

462

## 463 **4.2 Luminescence Dating**

464 Luminescence dating yielded ages between  $53.5 \pm 4.9$  and  $91.5 \pm 9.1$  ka (samples L-EVA 2010  
465 and 2022) (Figs. 2 and 7, Tab. 2). The dated layers 6 to 11, including the archaeological find  
466 horizons are well aligned chronologically. For find horizon Li-I (stratigraphic layers 7 and top  
467 of layer 8), the three samples (L-EVA 2014, 2015 and 2017) range between  $70.8 \pm 8.0$  and  $71.6$   
468  $\pm 7.0$  ka with a mean age of  $71.3 \pm 7.3$  ka. Find horizon Li-II (stratigraphic layer 11) gave an age  
469 between  $89.5 \pm 8.2$  and  $91.5 \pm 9.1$  ka and a mean age of  $90.5 \pm 8.7$  ka (samples L-EVA 2024  
470 and 2022). Sample L-EVA 2010, taken in a position where find horizon Li-I was cryoturbated  
471 upwards, gave a cryoturbation age of  $53.5 \pm 4.9$  ka. This is close to the previous TL-age of  $57$   
472  $\pm 6$  ka for this site (Veil et al., 1994). More details on data evaluation, equivalent dose ( $D_e$ )  
473 estimation and age calculation can be found in Supplementary Section 6.

474

## 475 **4.3 Palynology**

476 The pollen spectra and vegetation succession of sublayers 11a and 11b (incl. 11b<sub>2</sub>) from Trench  
477 2 (Fig. 2b, c; Supplementary Figures. S60 and S61) are quite similar. They contain about 80 to  
478 85% woody taxa (arboreal pollen, AP) consisting mainly of *Pinus* and *Betula* and very few  
479 *Alnus*, *Larix*, *Myrica*, *Juniperus* and *Picea*, while the NAP (non-arboreal pollen) are represented  
480 by Poaceae, Cyperaceae and heliophile herbs, which is indicative of a densely wooded boreal  
481 conifer forest. Sparsely occurring pollen of aquatic and wetland taxa like *Sparganium spec.*,  
482 respectively *Montia* indicate open water and swampy environments. In layer 10, the strong  
483 increase of Poaceae (40%), different NAP, and the drop of *Pinus* (15%) associated with *Betula*  
484 amounts of about 30%, and occurrences of the cryptogams *Ophioglossum* and *Selaginella*  
485 *selaginoides* are interpreted as a strong opening of the landscape towards a tundra-like  
486 vegetation. This sequence (layers 11a, 11b, 11b<sub>2</sub> and 10) is indicative of the late Brörup  
487 Interstadial, transitioning into the following Rederstall Stadial (Behre, 1989; Menke and Tynni,  
488 1984; Veil et al., 1994; Supplementary Section 7).

489

490 In core PD.028, the lower peat at 465-555 cm shows distinct interstadial conditions with AP  
491 spectra characterized by *Pinus*, *Betula*, *Picea* and *Larix*, which amount to 80-90%  
492 (Supplementary Fig. S62). A diverse heliophile pollen flora consisting of *Valeriana vulgaris*-  
493 type, *Matricaria*-type and *Artemisia* furthermore characterizes dry boreal forest habitats.

494 Both the sandy humiferous layer (355-390 cm) and the coarse detrital, peaty mud (230-  
495 250 cm) in superposition reveal pollen spectra dominated by NAP (up to 60%) with high  
496 amounts of Poaceae. The rich heliophile flora includes among others *Artemisia*, *Valeriana*  
497 *montana*-type, *Matricaria*-type, *Polygonum bistorta*-type, *Helianthemum oelandicum*-type,  
498 *Epilobium* and Chenopodiaceae. Among the wooden taxa, *Betula* reaches about 30%, whereas  
499 *Pinus* values have dropped down to <15%. The spectra therefore clearly reflect a phase of  
500 rather open landscape and dry and cold conditions, also indicated by the massive occurrence  
501 of colonies of the cold-tolerant green alga *Pediastrum kawraiskyi*.

502 The lowermost two bulk samples are correlated with the Odderade Interstadial, WF IVb  
503 (Behre, 1989; Menke and Tynni, 1984; Veil et al., 1994; Supplementary Figure S62), whereas  
504 the uppermost samples most probably represent early phases of the Schalkholz, WP I Stadial.  
505 Pollen diagrams and detailed interpretation are presented in Supplementary Section 7 and  
506 the main palaeoenvironmental results and biostratigraphical subdivision can be found in Tab.  
507 3 and Supplementary Tab. S14.

508

#### 509 **4.4 Micromorphology**

510 The analyzed sequence is dominated by quartz sand, common clay and rare inclusions of  
511 organic material and mica. Anthropogenic remains, flint and charcoal are rare and only occur  
512 in the lithofacies associated with the archaeological layers. The microstructure and fabric, i.e.,  
513 horizontal orientation of plant residues, channels filled with clay, and the good preservation  
514 of organic material indicate waterlain, potentially lacustrine environments with incipient soil  
515 formation (Bouma et al., 1990; Cohen, 2003; Taylor et al., 1998) for the lower part (layer  
516 11a/b, 10). In contrast, for the upper part (layers 9 to 5) of the sequence the  
517 micromorphological analysis does not allow a differentiation between waterlain and aeolian  
518 deposition. Turbation features are overall rare and limited to individual layers, indicating good  
519 integrity of the archaeological assemblage. We did not, however, sample and analyze the  
520 cryoturbated parts of the sequence. The upper find horizon, Li-I, is associated with a fine and  
521 compact lithofacies (layer 7), however, the origin of this compaction was not apparent in thin  
522 section. No cementation features were observed at this scale of observations, instead the  
523 grains appear as very densely packed with very limited void space. The overlying coarse-  
524 grained layer 6 shows intense clay illuviation with the compacted, fine grained layer 7  
525 presenting a barrier to the downward transportation of clay. This clay illuviation is not

526 associated with further soil formation features, and it is therefore unclear whether this clay  
527 illuviation represents a soil formation process and to what former surface this process may be  
528 connected. For more details, see Figures S 50 to S 55 and Supplementary Section 5.3.

529

#### 530 **4.5 Phytolith Analysis**

531 The ratio of grass short- to long-cells was measured to ascertain phytolith preservation, given  
532 that short-cells are more likely to preserve than long-cells due to their shape and higher  
533 silicification (Supplementary Table S16). Of the five analysed samples, MH3 and MH5 (layers  
534 7 and 9) showed lower ratios, which is suggestive of poorer preservation (Madella and  
535 Lancelotti, 2012). However, the rarity and widespread absence of dendritic long-cells indicate  
536 some taphonomic alteration in all samples. The ratio and the presence of dendritic long-cells  
537 in MH2 (layer 11a) indicates that this sample has the least taphonomic alternation. Long-cells,  
538 such as psilate and sinuate types, dominate all the assemblages, and are typical of monocot  
539 plants, particularly Poaceae. We also found many short-cells and some bulliforms, which again  
540 shows the presence of grasses as a vegetation component. Less important were phytoliths  
541 produced by eudicot shrubs and trees. These include the two main categories; wood/bark and  
542 leaves. Eudicot leaf types were found in MH4 (layer 8). Wood/bark types occur in MH2 (layer  
543 11a) and MH3 (layer 7). In addition, sclereids deriving from sclerenchyma were found in MH3  
544 (layer 7). Unspecific eudicot types were found in all samples, except MH5 (layer 9). This  
545 indicates the presence of a shrubby vegetation component. The relatively low total numbers  
546 in most of the samples imply a low bioproductivity with constrained growing conditions that  
547 deposited only few phytoliths. In that way, samples MH1 and MH3 to MH5 (layers 7 to 9) are  
548 very similar. In contrast, the far richer assemblage in MH2 (layer 11a) indicates warmer and  
549 wetter conditions that fostered a plant-rich environment, including grasses and woody plants  
550 (see Supplementary Tables S16, S17; Supplementary Section 8).

551

#### 552 **4.6 Grain size Analysis**

553 The 116 grain size fractions (0.04 - 2000  $\mu\text{m}$ ) for each sample were subjected to uni- and  
554 multivariate statistical analysis. Firstly, we calculated the sorting and the mean grain sizes  
555 (Blott and Pye, 2001; Folk and Ward, 1957) and displayed them as a scatter plot (Fig. 3a).  
556 Secondly, a principal component analysis (PCA) was conducted and the most significant  
557 principal components PC1 and PC2 were displayed, together accounting for 95.8% of the total

558 data variance (Fig. 3b). In both graphs, we assigned each sample to the sedimentological  
559 process identified during field descriptions (and micromorphological analysis, if applicable)  
560 and constructed convex hulls around all processual clusters. Both graphs differentiate well  
561 between the different classes formed during fieldwork, encompassing aeolian,  
562 niveofluvial/niveoaeolian, solifluctive and lacustrine processes. This satisfactory  
563 discrimination was unexpected, seeing that the Saalian glaciofluvial sediments as main source  
564 material for the analyzed slope deposits crop out <100 m upslope, and grain size sorting is i.a.  
565 a function of transport distance. Moreover, all classes in the graphs contain samples from  
566 Trench 1 (dots) and Trench 2 (triangles), providing further evidence that layers 3, 4, 5, 7 and  
567 9 can be directly correlated in both trenches (Figs. 2 and 3, compare Tab. 1). A more detailed  
568 evaluation and interpretation of the grain size data is provided in Supplementary Section 5.2.

569

#### 570 **4.7 Archaeology**

##### 571 ***Lichtenberg I***

572 During our initial survey in 2017, we found one Keilmesser (Fig. 4: 1) and one fragment of a  
573 bifacial tool (Supplementary Figure S1) in the cryoturbated layer 7' below the 1987-1993  
574 excavation trench. In the course of our fieldwork in 2019, we excavated 17 flakes (Fig. 4: 2-7)  
575 and three cores from Trench 1. One flake was found in the cryoturbated layer 7' (Fig. 2a), 12  
576 artefacts in layer 7 and seven artefacts in layer 8. All artefacts are made of Baltic Flint.  
577 Although being low in number and mostly typologically rather undiagnostic, finds like the  
578 Keilmesser from layer 7' as well as a relatively large flake that is potentially a product of bifacial  
579 reduction (Fig. 4: 6) helped, in addition to the sedimentological characteristics of the deposit  
580 (see section 4.1 above), to identify layer 7 as equivalent to the main find horizon of the 1987-  
581 1993 Keilmessergruppen assemblage (see Veil et al., 1994). One additional flake (Fig. 4: 8) was  
582 recovered from Layer 7 in Trench 2. This also supports an archaeological connection of the  
583 stratigraphies in Trench 1 and Trench 2.

584

585 *Lichtenberg I - Traceology.* Our preliminary traceological analysis (Supplementary Section 4,  
586 Supplementary Table S10) revealed neither use-wear traces on the two flakes analyzed, LIA-  
587 36 and LIA-50 (Fig. 4: 6, 7), nor on the bifacial tool fragment Li-6. For the analyzed Keilmesser  
588 Li-7 (Fig. 4: 1; Fig. 5), however, the wear traces suggest its use as a hafted butchering knife.  
589 The tool is made of dark Baltic Flint, and shows little signs of severe post-depositional

590 mechanical damage or chemical weathering that could have hindered the preservation of  
591 wear traces. Traces indicating the natures of the transformed material, however, are subtle  
592 and constricted to lightly developed micro polishes zones located on the distal portion of the  
593 working edge (Fig. 5a: F1). Negative edge rounding and additional polished surfaces are found  
594 further inwards on the dorsal side of the working edge (Fig. 5a: F2). Directional markers,  
595 including striations running parallel to the working edge of the tool and generally associated  
596 with lightly developed polished spots are also located on the dorsal surfaces of the working  
597 edge (Fig. 5a: F3 and F4). In combination with the micro negatives located on the ventral side  
598 of the tool (Fig. 5a: F5 and F6), a longitudinal cutting motion under the exertion of pressure  
599 is suggested, what is comparable with the interpretation of previous traceological analyses  
600 from Lichtenberg (Veil et al., 1994). The lightly-developed polish and the presence of striations  
601 on the analyzed specimen indicates the processing of a soft organic material and occasional  
602 contact with harder organic substance. Therefore, we suggest the use as butchering knife.

603

604 The back of Keilmesser Li-7 shows a series of marked modifications and traces that are  
605 associated with intense mechanical stress (Fig. 5b). The distal portion of the back shows  
606 marked rounding and crouching that are evident by short continuous micro-negatives with  
607 step and hinge terminations (Fig. 5b: F1 and F2). Bright and semi-undulating cohesive polished  
608 areas were identified on the edges of the negatives located on the medial portion of the back,  
609 indicating the repeated contact with a hard organic substance (Fig. 5b: F3). Together, these  
610 signs may indicate the continued mechanical friction of the tool with a hard organic haft, thus  
611 possibly indicating the use of composite tools by Neanderthals at Lichtenberg. Regarding the  
612 common interpretation that Keilmesser were handheld tools (e.g., Jöris, 2006), we do not  
613 suggest that Keilmesser tools were generally hafted. However, our results make it paramount  
614 to conduct further investigations into the subject.

615

## 616 ***Lichtenberg II***

617 We discovered 192 artefacts (Supplementary Table S3; Supplementary Table S9;  
618 Supplementary Datafile) in find horizon 11a (Fig.7). 173 artefacts are preserved in a fresh  
619 condition, 7 are rolled and 12 show light edge damage (see Supplementary Datafile). The  
620 assemblage is dominated by flakes, followed by cores and flake tools. The assemblage further  
621 includes shattered pieces and core tools. We also found three manuports and one piece that

622 was typed as 'other' which are most likely raw material imports and/or hammerstones. If we  
623 exclude manuports (n = 3), other (n = 1) and shatter (n = 25), the remaining assemblage of 163  
624 artefacts consists of 51.5% flakes (n = 84), 30.1% tools (n = 49) and 18.4% cores (n = 30).  
625 However, the category of tools also includes cores that were later transformed into tools, so  
626 that the original share of cores was higher (n = 42, see Supplementary Section 3.5, 3.7).  
627 Nevertheless, the share of tools is relatively high compared to Lichtenberg I (18.8% (Veil et al.,  
628 1994)).

629

630 *Lichtenberg II - Raw material.* The artefacts are made predominantly of Baltic Flint (n = 184;  
631 Supplementary Table S1). The raw material was of exceptionally small size, as is demonstrated  
632 by a controlled raw material sample from layer 11a that gave a median weight of 5.3 g  
633 (Supplementary Figure S33). Despite its small size, the flint was of rather good quality  
634 (Supplementary Table S2). Only one large core (Fig. 4: 20) shows internal cracks and flaws that  
635 hampered the core reduction and led to unexpected breaks of the resulting flakes. 14 (7.3%)  
636 artefacts show thermal alterations (Fig. 4: 10, 16; Supplementary Table S2), indicating the  
637 presence of artificial or natural fires at the site. Additionally to flint, six artefacts were made  
638 of quartzite (Fig. 4: 21).

639

640 *Lichtenberg II - Size.* The artefacts from Li-II are relatively small. Their median dimensions  
641 (either longest width or length) range between 19.48 mm for the flakes and 27.54 mm for the  
642 cores (Supplementary Table S5). Comparing the flakes from this site to 14 Central European  
643 assemblages ranging from the Eemian interglacial to early MIS 3, Li-II has the smallest artefacts  
644 (Supplementary Figure S36). Exceptional are the core LIA-335 (Fig. 4: 20), the quartzite flake  
645 LIA-513 (Supplementary Figure S41), and the quartzite flake tool LIA-504 (Fig. 4: 21). With their  
646 maximum dimensions of 114.7 mm, 106.3 mm, and 75 mm respectively, these by far exceed  
647 the median dimensions of the assemblage.

648

649 *Lichtenberg II - Cores* Fig. 4: 19,20; Supplementary Section 3.5). In the following analysis, we  
650 additionally included those cores that were later transformed into tools (see below). Most  
651 of the cores were only knapped up to half of their surface (72.5%, n = 29). Predominantly, the  
652 cores were exploited on a single (47.5%, n = 19) or two flaking surfaces (32.5%, n = 13). The  
653 angles between the striking platform and the flaking surface have a median value of 88° (min

654 = 64°, max = 108°, sd = 8.75). 35% (n = 14) of the cores have only one single flake scar, but 3 -  
655 5 flake scars are common as well (in total 52.5%, n = 21). At a significance level of p = 0.05, a  
656 linear model (Supplementary Figure S37) reveals a weak significant relationship between core  
657 lengths and the number of flake scars (Multiple R-squared: 0.12, Adjusted R<sup>2</sup>: 0.099, F-statistic:  
658 5.312 on 1 and 38 DF, p-value: 0.03). This implies that larger cores have tentatively more flake  
659 scars and were thus exploited more intensively. In turn, the small raw material size tentatively  
660 led to low exploitation values on the small cores. Taking all flaking surfaces together, most  
661 cores were knapped unidirectionally (80.6%, n = 54). Most striking platforms consist of a  
662 natural (51.3%, n = 20) or plain (43.6%, n = 17) surface, whereas fine preparation of striking  
663 platforms does not occur in the assemblage. In conclusion, simple flaking methods dominated  
664 the blank production in Lichtenberg II. Core preparation was not common, if not entirely  
665 missing. The simple cores, sometimes just flaked once, may also be due to the small raw  
666 material size, as some nodules make only one-time flaking possible.

667

668 *Lichtenberg II - Flakes* (Fig. 4: 15, 22; Supplementary Section 3.6). We included 55 complete  
669 flakes into the analysis, as not all variables are preserved on flake fragments. The platform  
670 attributes reinforce the observation made on the cores that striking platform preparation (i.e.,  
671 Levallois *sensu largo*) was not common, as platforms with natural (21.8%, n = 12) and plain  
672 surfaces (50.9%, n = 28) dominate the flake assemblage. Platforms that crushed during  
673 knapping also have a relatively high share of 23.6% (n = 13). The EPA has a median value of  
674 85° (min = 58°, max = 109°, sd = 10.85°), comparable to the flaking angles observed on the  
675 cores. Most of the flakes originate from an advanced state of core reduction, as the share of  
676 fully cortical flakes is low (15.1%, n = 8). This may be a reasonable number, as cores naturally  
677 produce a lower share of fully cortical flakes than flakes with no or only remnants of natural  
678 surfaces. However, if we sum up all the flakes with remnants of natural surfaces on their dorsal  
679 face, we end up with 62.2%. This is more than half of the flake population and may be caused  
680 by the small size of the raw material. The observed dorsal scar directions on the flakes show  
681 the tendency that the blank production in Li-II was dominated by unidirectional flaking (51.1%,  
682 n = 23). This confirms the similar observation made on the cores.

683

684 *Lichtenberg II - Tools* (Tab. 4, Fig. 4: 9-14, 16-18; Supplementary Section 3.7). The tools from  
685 Lichtenberg II show a high typological diversity. They are dominated by flakes that were

686 potentially used (Fig. 4: 9,17), tools with partial or limited edge retouch (Supplementary Figure  
687 S39) and endscrapers (Fig. 4: 12,13). They were manufactured from a diversity of blanks, such  
688 as natural pieces, cores and flakes, and are dominated by the latter (62.5%, n = 30).  
689 Endscrapers and endscraper combination tools were manufactured from thick blanks (Fig. 4:  
690 12, 13; Supplementary Table S8), indicating special functional requirements. In addition, a  
691 rather steep endscraper edge can only be produced on a relatively thick blank. The high share  
692 of cores (25%, n = 12), as well as two shattered pieces that also served as blanks for tools,  
693 indicate the high importance of recycling within the Li-II assemblage. For example, the artefact  
694 LIA-379 was initially a core and then transformed into a hammerstone (Supplementary Figure  
695 S38). The traceology (see below) indicates that tool functions go beyond the current  
696 typological classifications and descriptions.

697

698 *Lichtenberg II - Traceology* (Fig. 6). The preliminary traceological analysis (Supplementary  
699 Section 4, Supplementary Table S10) of lithic material from Li-II indicates a heterogeneous  
700 pattern of activities, including the processing of soft animal materials, soft and abrasive  
701 vegetable materials and hard vegetable materials (wood). Notable are the traces located on  
702 the ventral distal working edge of artefact LIA-550 (Fig. 4: 9; Fig. 6a). They show a well-  
703 developed bright undulating polish with a high incidence of directional markers, indicating a  
704 crossed transverse motion. This bright well-developed polish likely formed by the contact with  
705 a highly abrasive and soft vegetal material, while the striations may be related to the  
706 admixture of mineral particles, possibly sand or grit, during scraping activity. The resemblance  
707 to cereal polish is remarkable (Clemente and Gibaja, 1998), indicating the working of silicate-  
708 rich grasses or sedges. The combination of percussive and pressure force was also found on  
709 the Li-II artefacts as well as the possible use of hafting technology. The latter was observed on  
710 artefact LIA-307 (Fig. 4: 12; Fig. 6b) based on the presence of G type polish (Moss, 1987; Rots,  
711 2010) and the scarring on the dorsal surface along the edges of the central negatives. The  
712 general small-artefact characteristics of the assemblage, together with the high incidence of  
713 crushing, coupled with the high amount of force used during the different productive activities  
714 undertaken at the site, may suggest that artefact LIA-307 was not the only hafted tool. The  
715 absence of further hafting wear, however, constrains the further exploration of this possibility.

716

717

718

719 **5. Discussion**

720 **5.1 Comparison with previous geochronological data**

721 Stratigraphic layer 7 (find horizon Li-I) is locally deformed upwards by cryoturbation, especially  
722 injection, but is still associated with lithic finds there (Fig. 2). To get an impression of the timing  
723 of deformation, we dated this cryoturbated sediment with luminescence and obtained an age  
724 of  $53.5 \pm 4.9$  ka (L-EVA 2010, Fig. 7). This compares very well to the previous TL-age of  
725  $57 \pm 6$  ka for the find horizon Lichtenberg I (Veil et al., 1994). The origin of our sample from a  
726 cryoturbated context allows the following conclusions: (i) The previous age must likewise have  
727 been obtained from a cryoturbated deposit. This is supported by the fact that during the  
728 former excavation, a depth of ca. 1.2 m below surface was usually not exceeded. Our  
729 excavations revealed that in these higher stratigraphic positions only cryoturbated  
730 expressions of the find horizon occur (Fig. 2). (ii) In spite of considerable progress in  
731 luminescence dating during the last decades concerning measurement protocols and targeted  
732 signals (Buylaert et al., 2012; Murray and Wintle, 2003; Wintle and Adamiec, 2017), the  
733 similarity of the previous and newly-presented luminescence ages attest the remarkably high  
734 reliability of the former TL dates. Therefore, only lithostratigraphic challenges – i.e. the  
735 cryoturbations – apparently hindered a more accurate temporal estimation of the deposition  
736 and occupation at that time. (iii) The two dates imply a cryoturbation age that is time-  
737 equivalent to the early MIS 3. Even though permafrost – the probable driver for these  
738 deformations – was more widespread and effective in Central Europe during MIS 4 and MIS 2  
739 (Bertran et al., 2014), it is known to have existed in MIS 3 as well (e.g. Van Huissteden et al.,  
740 2003; Van Meerbeeck et al., 2011). However, active permafrost is not a prerequisite for the  
741 partial deformation/injection of the find horizon Li-I. Instead, this can also be a function of  
742 loadcasting or cryogenic pressure during thaw degradation of the permafrost, which would be  
743 in agreement with the two independent ages suggesting a deformation during the more  
744 temperate early MIS 3 (French, 2008; Vandenberghe, 2013; Vandenberghe and Van den  
745 Broek, 1982). Nonetheless, according to our current state of knowledge, a cryoturbation age  
746 falling within the later MIS 3 or even MIS 2 cannot be completely ruled out. Therefore, a  
747 follow-up study will deal with the cryogenic capping sediments in Lichtenberg.

748

749

750

751 **5.2 Comparison with global paleoclimate records**

752 ***Find horizon Li-II***

753 For layer Li-II, corresponding with stratigraphic layer 11a, two very similar luminescence ages  
754 from samples L-EVA 2022 and 2024 ( $91.5 \pm 9.1$  ka and  $89.5 \pm 8.2$  ka) gave a mean age of  $90.5$   
755  $\pm 8.7$  ka. In the palynological data, we observe temperate, late interstadial conditions,  
756 characterized by an opening boreal pine-birch forest in layers 11a and the lower part of 11b,  
757 assigned to the Brörup Interstadial WE IIb (Tab. 3, Supplementary Section 7) (Behre et al.,  
758 2005; Behre and Lade, 1986; Menke and Tynni, 1984; Veil et al., 1994). The environment  
759 changed toward heliophyte and grass-rich, cold-stage tundra vegetation in the following  
760 Rederstall Stadial. In our sequence, this shift happens abruptly between layers 11a and 10, but  
761 gradually to the top of layer 11b. Therefore, the occupation of find horizon Li-II should have  
762 occurred during late phases of the Brörup Interstadial, whereby the obtained mean age of  
763  $90.5 \pm 8.7$  ka represents this terminal phase (Fig. 7). Compared with global paleoclimate  
764 records, this age for the end of Brörup Interstadial corroborates the correlation with the end  
765 of MIS 5c (peak at 96 ka in Lisiecki and Raymo (Lisiecki and Raymo, 2005b)) and with Greenland  
766 Interstadial (GI) 22 in the synchronized Greenland ice core records, dated to about 89 ka at its  
767 peak (Rasmussen et al., 2014). To our knowledge, for the Brörup Interstadial no direct  
768 numerical dates exist in its type region on the northern Central European Plain so far.  
769 Luminescence ages similar to ours for the end of equivalent interstadials have been obtained  
770 from loess records of Northern France at ca. 85 ka (Antoine et al., 2016) and Dolní Věstonice  
771 (CZ) at ca. 90 ka (Antoine et al., 2013; Fuchs et al., 2013). In the Alpine Foreland, the peak of  
772 the Brörup equivalent has been dated to around 96 ka (compiled by Preusser, 2004) and its  
773 end to ca. 89 ka in the highly-precise NALPS speleothem record (Boch et al., 2011). Altogether,  
774 these dates support our finding that the end of the Brörup Interstadial (mean age of  
775  $90.5 \pm 8.7$  ka in Lichtenberg) coincides with GI 22 and the termination of MIS 5c.

776

777 ***Find horizon Li-I***

778 In find horizon Li-I (stratigraphic layers 7 and 8), three nearly identical luminescence ages for  
779 samples L-EVA 2014, 2015 and 2017 ( $71.6 \pm 7.0$  ka,  $71.5 \pm 7.0$  ka and  $70.8 \pm 8.0$  ka) gave a  
780 mean age of  $71.3 \pm 7.3$  ka. Regarding lithostratigraphy, Li-I is under- and overlain by cold stage  
781 deposits (section 4.1, Supplementary Section 5.1), and the covering layers show clear  
782 permafrost features. This suggests a pre-pleniglacial age for Li-I (Jöris, 2004), because

783 permafrost rarely occurred in Central Europe before MIS 4 (Bos et al., 2001; Vandenberghe  
784 and Pissart, 1993). Our chronostratigraphy implies that layer 9 (mean age of  $72.5 \pm 7.8$  ka) is  
785 only slightly older than layers 7 and 8. Furthermore, as evidenced by the alternating deposition  
786 of layers 7 and 9 in the stratigraphy of Trench 2, these partially even occur contemporaneously  
787 (Fig. 2c). Accordingly, comparable cold-stage conditions for the formation of layers 7 to 9 are  
788 also suggested by similar phytolith results (section 4.5, Supplementary Section 8), which point  
789 to a grass-rich vegetation in these layers. However, layers 7 to 9 were pollen-sterile in the  
790 trenches, thus hindering their direct biostratigraphical assignment. In contrast, reliable  
791 information was obtained from core PD.028, directly south of Trench 1 (Figs. 1, 7): (i) A thick  
792 peat layer directly below the niveofluvial sands of layer 9 was characterized by dense *Pinus-*  
793 *Betula* forest, being characteristic for the Odderade Interstadial WE IVb (Tab. 3,  
794 Supplementary Section 7) (Behre et al., 2005; Behre and Lade, 1986; Menke and Tynni, 1984;  
795 Veil et al., 1994). Based on the bio-/lithostratigraphy and the luminescence ages for the  
796 overlying layers 8 and 9, we correlate the Odderade peat with GI 21 (Jöris, 2004; Stephan,  
797 2014). (ii) Unlike in the trenches, the cold stage niveofluvial sands of layer 9 showed two  
798 interbedded organic-rich layers that were characterized by a grass- and heliophyte-rich open  
799 vegetation belonging to the early Schalkholz, WP I Stadial (Tab. 3, Supplementary Figure S62,  
800 Supplementary Tab. S14).

801 On the premise that these two organic-rich sediments represent low-magnitude climatic  
802 ameliorations (Hahne et al., 1994; Vandenberghe and van der Plicht, 2016), we cautiously  
803 regard them as minor interstadial oscillations seldomly described for Northern Germany  
804 (Supplementary Section 7). These minor oscillations following the Odderade, stratigraphically  
805 could be associated with GI 20 and 19 (Rasmussen et al., 2014), which would also agree with  
806 the mean luminescence age of layer 9 of  $72.5 \pm 7.8$  ka (with a tendency to increase with depth,  
807 see Fig. 7). As for the find horizon Li-I, its mean luminescence age of  $71.3 \pm 7.3$  ka and its  
808 superposition above the minor interstadial oscillations suggests correlation with Greenland  
809 *Stadial* (GS) 19 (Rasmussen et al., 2014).

810 Much like the Brörup, to our knowledge the Odderade Interstadial is mostly lacking an  
811 independent chronology in the type region of northern Central Europe, apart from previous  
812 dating attempts with  $^{14}\text{C}$  (Behre and van der Plicht, 1992; Grootes, 1978) and unpublished  
813 luminescence ages, obtained by Thiel at the site of Osterbylund (Stephan et al., 2017). For  
814 Northern Germany, the Odderade was recently correlated with Greenland Interstadial (GI) 21

815 (Stephan, 2014). At a few sites (namely Keller, Schalkholz and Osterbylund), above the  
816 Odderade layer, but below the deposits of the first glacial maximum (~MIS 4), one or two weak  
817 Podzol paleosols exist, representing a slight climatic amelioration phase (Keller-Interstadial),  
818 ascribed to GI 20 and 19 (Menke, 1976; Stephan, 2014). Our chronological correlations  
819 compare very well with this northern German stratigraphy, but also with independently-dated  
820 loess and pollen/speleothem records in neighboring regions: Antoine et al. (2016) also  
821 correlated the Odderade/St. Germain II soils with GI 21 for the loess-paleosol-sequences in  
822 northern France and report this phase to end at ca. 80 ka. Above the Odderade/St. Germain  
823 II, there are two paleosols (Ognon I and II) relating to GI 20 and GI 19. The conclusion of this  
824 soil formation has been dated to ca. 71 ka (ibid.). Similarly, two paleosols in the loess-paleosol-  
825 sequence of Dolní Věstonice in the southeastern Czech Republic were dated to  $73.1 \pm 4.7$  and  
826  $71.3 \pm 4.9$  ka, respectively, and were correlated with GI 20 and GI 19 (Antoine et al., 2013).  
827 Likewise, one or two minor interstadials in palynological records of South-Western Europe and  
828 southern Germany above the St. Germain II/Odderade Interstadial (e.g. Woillard, 1979) were  
829 ascribed to GI 20 and 19 (Ognon I/II and Dürnten), and the latter was dated to ca. 73 ka (Müller  
830 and Sánchez Goñi, 2007). Furthermore, in the NALPS speleothem record of the northern Alps,  
831 a minor interstadial related to GI 19 yielded an age of ca. 72 ka (Boch et al., 2011). Although  
832 for the Lichtenberg record, numerical dating of the Odderade peat and the overlying two  
833 minor interstadials cannot be presented yet, our chronological and biostratigraphic  
834 framework suggests their close coupling to the Greenland Interstadials GI 21 to 19.  
835 Consequently, the mean age ( $71.3 \pm 7.3$  ka) of the overlying find horizon Li-I (correlated with  
836 GS 19) represents a plausible age for the inception of the MIS 4 pleniglacial. Comparing our  
837 record with the marine chronology (Lisiecki and Raymo, 2005b), we regard the Odderade peat  
838 (GI 21) and the overlying two minor interstadials (GI 20 and 19) of core PD.028 to be part of  
839 MIS 5a, whereas stratigraphic layers 8 and 7 (find horizon Li-I, GS 19) are tentatively assigned  
840 to early MIS 4. This implies that the upper boundary of the Odderade Interstadial is not  
841 congruent with the end of MIS 5a, in this region (Behre, 1989a; Jöris, 2004; Stephan, 2014).

842

### 843 **5.3 Site formation, paleoenvironment and humans**

844 Neanderthals occupied the northern site of Lichtenberg during the Eemian (Hein et al., 2021),  
845 the following early Weichselian Brörup Interstadial (find horizon Lichtenberg II), through to  
846 the onset of the first Weichselian glacial maximum (find horizon Lichtenberg I). In the

847 following, we will connect our sedimentological/paleoenvironmental and archaeological  
848 results to draw inferences about past human behavior in changing environments in  
849 Lichtenberg.

850

### 851 ***Lichtenberg occupation during the Mid-Eemian***

852 Near the south-facing shore of a small lake, a half-bog formed just above the groundwater  
853 level during the mid-Eemian Interglacial (pollen zone E IVb/V). This was the time and position  
854 for Neanderthal occupation, as inferred from few artefact finds (2 flakes and a few small chips  
855 and fragments) within the core PD.030 (Hein et al., 2021). A densely-forested landscape was  
856 reconstructed for the area (>95% arboreal pollen), dominated by hazel (*Corylus*), alder (*Alnus*),  
857 lime (*Tilia*) and hornbeam (*Carpinus*), with the admixture of further thermophile taxa, such as  
858 elm (*Ulmus*), oak (*Quercus*) and yew (*Taxus*). Among the indicators for local swampy  
859 conditions are palynomorphs of ferns (*Polypodiaceae*), cattail (*Typha*) and bur-reed  
860 (*Sparganium*) (Behre, 1989; Menke and Tynni, 1984).

861 This fully-forested landscape contrasts with other contemporaneous Eemian sites from drier  
862 regions of central Germany (Gaudzinski-Windheuser and Roebroeks, 2014; Litt and Weber,  
863 1988; Toepfer, 1958; Weber, 1990), where last interglacial Neanderthals are assumed to have  
864 lived in semi-open landscapes (Pop and Bakels, 2015). Thus, contrary to earlier hypotheses  
865 (Pop and Bakels, 2015), we suggest that the Lichtenberg-Eemian Neanderthals adapted well  
866 to wooded paleoenvironments. However, so far we have too few artefacts to draw inferences  
867 about Neanderthal behavior in Lichtenberg during the last interglacial. Therefore, future  
868 excavations are planned to reveal more about the structure and spatial pattern of the Eemian  
869 settlement at the Lichtenberg lakeshore.

870

### 871 ***Li-II: Late Brörup Interstadial to Rederstall Stadial***

872 During the Brörup Interstadial a beach sediment (layer 11a) was deposited at the shoreline of  
873 a small lake (ca. 1.5 km<sup>2</sup>, cf. Hein et al., 2021) with fluctuating water tables. In the late  
874 interstadial the water table was rising, as evidenced by the formation of a peaty deposit (layer  
875 11b) partially covering the beach, but also interfingering with its deposits. Such a hydrological  
876 shift is typical for transitional phases between forested and unforested periods due to the loss  
877 of woodland and associated decreasing evapotranspiration values (Behre et al., 2005; Tucci et  
878 al., 2021). Vegetation was characterized by boreal forests, with pine (*Pinus*) and birch (*Betula*)

879 being the main tree species (Caspers and Freund, 2001). Likewise, phytolith analysis indicates  
880 a relatively high bioproductivity (section 4.5). On the beach, local sandy to humic open stands  
881 were dominated by wet meadows, fern and heathland, and a diverse heliophytic flora. For the  
882 peaty deposit, we conclude there was a shallow water body with swampy conditions that  
883 featured rich stands of cattail (*Typha latifolia* type), reed and sedges. In this environment, the  
884 occupation of Li-II took place directly by the shoreline. Regular occurrence of macroscopic and  
885 microscopic charcoal fragments (Supplementary Sections 5.3 and 7.2) document episodic  
886 burning events, either in connection with natural wildfires or Neanderthal fire use (Dibble et  
887 al., 2018; Glückler et al., 2021; Roebroeks et al., 2015). For the site of Gröbern (Central  
888 Germany), reconstructed summer temperatures of ca. 16°C and winter temperatures of ca. -  
889 15°C in the late Brörup (Kühl et al., 2007) demonstrate a highly continental climate that was  
890 caused by a lower sea level at that time (Lambeck, 2004). During the late Brörup stage WE IIb  
891 transitioning into WE III, the local water table in Lichtenberg kept rising as the woodlands  
892 gradually opened up and gave way to more heliophilous plants. Wave activity on the beach  
893 reworked plant material, charcoal and also small lithic fragments, thereby creating distinct  
894 driftlines. Eventually, during Rederstall Stadial, vegetation had changed into a grass- and  
895 heliophyte-rich tundra. The former beach was largely inundated by the rising lake level due to  
896 starkly decreased evaporation values in this non-forested environment (Behre et al., 2005).  
897 Subsequently, stadial conditions are recognized in the muddy shoreface deposit of layer 10  
898 and the uppermost part of layer 11b. Layer 10 emerges from layer 11b, that unconformably  
899 overlies layer 11a, and wedges out toward higher ground. This suggests that the top of layer  
900 11a might have been eroded prior to being covered.

901

#### 902 ***Li-I: Odderade Interstadial to early Schalkholz Stadial***

903 Within our record, the Odderade Interstadial is only detected in core PD.028 on account of  
904 higher accommodation space in the basin, south of the alluvial fan (Fig. 1, Supplementary  
905 Figure S49). However, the Odderade was also represented in the previously investigated core  
906 Veil 1, only about 10 m apart from core PD.028 (Veil et al., 1994). In both parallel cores, the  
907 Odderade peat occurs at the same depth, marking the ground water/lake level of that time.  
908 Vegetation was characterized by a dry boreal pine-birch forest with admixed spruce, juniper  
909 and larch. A rich but subordinate herbal flora indicates open stands nearby. Main peat formers  
910 were likely sedges and ferns. Following the Odderade, in the earliest Schalkholz Stadial,

911 niveofluvial slope deposition started, triggered by annual snow melt in a sparsely vegetated  
912 landscape (Christiansen, 1998b, 1998a). The grain size data show a coarsening trend from fine-  
913 sandy, slightly silty and slightly humic deposits above the Odderade peat in core PD.028 to the  
914 fine/medium sandy sediments of layer 9 in both the core and the trenches, and finally to more  
915 gravelly layer 8. This coarsening possibly indicates a raise of base level caused by a rising lake  
916 level. In our trenches, these niveofluvial sediments (layers 9 and 8) form a relatively coherent  
917 unit, but in core PD.028 with larger accommodation space, they are interbedded with two  
918 organogenic and lacustrine deposits. These attest to a continuously rising water level,  
919 interrupted by longer spells of relative landscape stability that were induced by denser  
920 vegetation. Stability would have slowed down the lake level rise and niveofluvial slope wash  
921 alike, and allowed these lacustrine/organic-rich deposits to form. Therefore, we regard these  
922 to represent minor local interstadial oscillations (see section 5.2, Supplementary Section 7).  
923 The dominating vegetation type during both oscillations indicates an open, grass-rich habitat.  
924 Among the woody taxa, *Betula* (likely dwarf birch), juniper and heath species, such as *Calluna*,  
925 *Empetrum* and *Vaccinium* stand out. Because these minor interstadial oscillations have not  
926 yet been described for Northern Germany by palynological findings, no direct  
927 paleotemperature estimation exists. However, in the Alpine Foreland, based on a chironomid  
928 record at the site of Füramoos, summer temperatures between 9-11°C were reconstructed  
929 for the two-part Dürnten Interstadial, the latter correlated with GI 19 (Bolland et al., 2021).  
930 For Northern Germany, the pleniglacial Oerel Interstadial (WP II) shows a similar pollen  
931 spectrum to those oscillations in Lichtenberg, hence, the reconstructed mean summer and  
932 winter temperatures for Oerel (9°C and -17°C) might be a fair approximation (Walkling, 1997).  
933 In Lichtenberg, at the culmination of lake level rise after the Odderade, large parts of the study  
934 area were inundated and an organic-free, thin, muddy shoreface sediment was deposited  
935 (layer 7). This is only missing at the higher ground in the northern part of Trench 2, which was  
936 not flooded apparently. Direct pollen information is lacking in this lacustrine deposit, but the  
937 results of phytolith analysis provide evidence that the conditions of layer 7 resembled those  
938 of the cold-stage, sparsely-vegetated niveofluvial layers 8 and 9 (section 4.5, Supplementary  
939 Section 8). Neanderthal occupation of Li-I (layer 7 and top of layer 8) occurred after the upper  
940 minor interstadial oscillation in a severely cold environment, as is further proposed by the  
941 modelled annual mean temperature (Gamisch, 2019a, 2019b) displayed in Figure 8b. We  
942 suggest that the occupational surface was topmost layer 8 near the lake shoreline. The

943 artefacts must have been smoothly embedded by the muddy shoreface sediments of layer 7  
944 during lake level rise, leaving no distinct taphonomical marks on the lithic finds.

945

946 ***Comparing Li-II to Li-I: Human behavior in changing environments***

947 The Lichtenberg find horizons represent two distinct site types, connected to different  
948 paleoenvironments and climatic conditions (Fig. 8b). Li-I and Li-II differ in raw material  
949 attributes and use, artefact size, as well as blank production, typology, and tool use.

950

951 Lichtenberg II has a high typological tool variability (Tab. 4, Fig. 4, Fig. 6). Edges with different  
952 functionalities on some artefacts (Supplementary Table S10) demonstrate that the tools often  
953 had several use-cycles. Further evidence for this recycling behavior comes from the cores and  
954 shattered pieces that were also recycled to tools. Traceology further suggests that the Li-II  
955 Neanderthals exploited the still richly-vegetated environment of late MIS 5c, and processed  
956 wood, plants, and other soft and hard organic material. All these assemblage characteristics  
957 indicate a longer and/ or repeated stay(s) at the lakeshore with a variety of domestic activities.  
958 Under these still temperate continental conditions at the lakeshore, we see the use of small  
959 and diverse raw material, what was possibly linked with the lack of accessible natural  
960 resources. We argue that relatively stable and densely vegetated landscape surfaces inhibited  
961 sediment erosion and favored weathering, and thus reduced the availability of fresh flint from  
962 the surrounding Saalian glacial deposits (Supplementary Section 3.4.4). Recycling and  
963 intensive tool use can also be related to this shortage of high-quality and large sized raw  
964 material. Faced with small and low-quality raw material in a forested landscape, Neanderthals  
965 at the site displayed an economic raw material management behavior. This may also explain  
966 the lack of more complex blank production techniques (e.g., Levallois, and/or discoidal  
967 methods), as the small-sized nodules in Li-II potentially did not allow for extensive core  
968 preparation (see for comparison Pop, 2014). Neanderthals mostly knapped small flint pieces  
969 a few times to obtain some larger flakes for further use, and/or to establish working edges on  
970 natural flint pieces. This behavior, as well as the small artefact size, the typological variety of  
971 tools and the recycling behavior are also known from the Eemian site of Neumark-Nord 2/2  
972 (Pop, 2014), as well as from the subsequent MIS 5c or 5a (Richter and Krbetschek, 2014; Strahl  
973 et al., 2010) assemblage Neumark-Nord 2/0 (Laurat and Brühl, 2021, 2006). It seems that  
974 forested to semi-open landscapes (Pop and Bakels, 2015), temperate organic rich

975 environments, as well as lakeshore areas with limited raw material availability, probably  
976 induced similar Neanderthal settlement behavior and resource management strategies on the  
977 northern European Plain between the Eemian and late MIS 5. However, besides  
978 paleoenvironmental triggers, we cannot rule out certain techno-cultural influences on the  
979 presence of typologically diverse small tool assemblages in Central Europe during the early  
980 last glacial, as these are also found in probably paleoenvironmentally slightly different, more  
981 southern regions of Central Europe. Examples are the lower layers of the Sesselfelsgrötte  
982 (Weißmüller, 1995), Bavaria/ Germany, and in layer 11 of the Kůlna Cave (Moncel and Neruda,  
983 2000; Valoch, 1988), Czech Republic. Based on these typological similarities, Li-II fits well into  
984 early last-glacial technocomplexes of Central Europe.

985  
986 In contrast to Li-II, the Li-I artefacts were exclusively manufactured on large, high quality flint  
987 pieces, such as frost shards that could be recovered in this area (Veil et al., 1994). This  
988 coincides with a sparsely-vegetated landscape, fostering sediment redeposition and providing  
989 freshly eroded flint from the Saalian glacial deposits (<100 m upslope). As suggested by former  
990 use-wear and techno-functional analyses (Veil et al., 1994; Weiss, 2020), the majority of Li-I  
991 tools served mainly for cutting soft tissue, potentially meat (Veil et al., 1994). This usage of  
992 Keilmesser as cutting tools confirmed by our traceological analyses of the Keilmesser Li-7 (Fig.  
993 4: 1). Furthermore, we recently showed (Weiss, 2020) that the Li-I Keilmesser were mostly  
994 discarded shortly before the edge angle of the working edge exceeded 60° (Gladilin, 1976), in  
995 other words, when the Keilmesser subsequently lost their functionality as cutting tools. In  
996 general, the functional focus of the Li-I tools led to a relatively low typological diversity in the  
997 presence of scrapers, bifacial scrapers, handaxes and Keilmesser. Based on the lack of cores  
998 and primary blank production in the assemblage, artefact refits that evidence on-site tool  
999 production, and the use-wear traces related to butchering activities (Veil et al., 1994), we  
1000 suggest a short-term occupation event at the lakeshore with a specialized objective, i.e., a  
1001 hunting/ butchering stay.

1002  
1003 Altogether, Li-I most probably represents a single, short-term event related to butchering  
1004 activities in a harsh and cold environment. In contrast, Li-II is interpreted to result from  
1005 repeated and probably longer stays at the lakeshore under still temperate continental climatic  
1006 conditions, with a variety of activities that were carried out at this site.

1007

1008 **5.4 Northern Neanderthals in the cold: occupations between MIS 5a and early MIS 3**

1009 From the last interglacial through to the end of MIS 5a/early MIS 4, the paleoenvironment of  
1010 the European Plain gradually changed from temperate towards colder climatic conditions and  
1011 open landscapes (Fig. 8b) (Caspers and Freund, 2001). The same trend is also documented in  
1012 the sediment sequence of Lichtenberg (see above). Besides the subsequent replacement of  
1013 the Eemian interglacial fauna by the mammoth fauna after the Eemian, we also expect to see  
1014 a shift from a more local roaming behavior (Kindler et al., 2020) of the potential prey species  
1015 to large herds with extended seasonal migration ranges. These changes and shifts in climate,  
1016 paleoenvironment and the fauna coincided with a shift in the archaeological record of  
1017 northern Central Europe. The early last-glacial small-tool assemblages such as those of Li-II  
1018 gradually disappeared. On the other hand, we see that in the upper part of the lower layers in  
1019 Sesselfelsgrötte or in Neumark-Nord 2/0 (Laurat and Brühl, 2021, 2006) bifacial tools, like  
1020 Keilmesser start to appear in low frequencies. This transition ended during MIS 5a with the  
1021 appearance of the late Middle Paleolithic Keilmessergruppen (Hein et al., 2020; Jöris, 2004;  
1022 Mania, 1990) that persisted in northern and eastern Central Europe until the early MIS 3 (Fig.  
1023 8a) (Jöris, 2004; Richter, 2016; Weiss, 2015), and probably extended as far east as the Altai  
1024 Mountains (Kolobova et al., 2020). Based on the short-term nature of their sites (Picin, 2016),  
1025 land-use systems with scattered special task and ephemeral camps (Richter, 2016, 1997), as  
1026 well as raw material transport over large distance in Central Europe (Féblot-Augustins, 1993),  
1027 the Neanderthals of the Keilmessergruppen are interpreted as highly mobile groups. This is  
1028 further expressed by the assumed mobile nature of the Keilmesser itself, enabling their long-  
1029 term use and transport through special re-sharpening possibilities (Iovita, 2010; Jöris, 2012,  
1030 2004; Weiss, 2020). Our evidence for hafting the Li-I Keilmesser supports this interpretation  
1031 of a tool concept with a long use-life.

1032 As Keilmessergruppen Neanderthals of Li-I were present in the northern latitudes at the onset  
1033 of the cold climatic MIS 4 (GS 19), we suggest that the increased residential and long-distance  
1034 mobility inferred from the Keilmessergruppen assemblages is one aspect of Neanderthal  
1035 behavioral adaptations to the cold climate and the related paleoenvironmental conditions. In  
1036 contrast to this, although last interglacial Neanderthals are also interpreted as highly mobile,  
1037 it was inferred from the archaeological and faunal assemblage of the Eemian site Neumark-

1038 Nord 2/0 (Kindler et al., 2020) that their mobility must have been more local instead of  
1039 travelling large distances.

1040 As mentioned above, the site Salzgitter-Lebenstedt is another proof of Neanderthals living  
1041 under cold climatic conditions, as the find layers contain remains of a cold climatic vegetation  
1042 (Pastoors, 2001; Pfaffenberg, 1991; Selle, 1991). Furthermore, that sequence shows a  
1043 succession from subarctic (find horizon) to arctic conditions (silts covering the find horizon)  
1044 (Pfaffenberg, 1991; Selle, 1991), comparable to the sediment sequence of Li-I. Given our  
1045 paleoenvironmental results and the age of Li-I, the formerly suggested MIS 5a/4 (Jöris, 2004)  
1046 age for Salzgitter-Lebenstedt seems very plausible by analogy. This implies a repeated or  
1047 continuous Keilmessergruppen Neanderthal occupation of cold climatic northern latitudes  
1048 with specific adaptations to these environments, like e.g., seasonal hunting of migratory game  
1049 herds, such as late summer/ early autumn reindeer hunting, as evidenced in Salzgitter-  
1050 Lebenstedt (Gaudzinski, 1999, 1998). The latter suggests that late Neanderthals stayed at least  
1051 until early autumn in northern regions of Central Europe. But even for that season,  
1052 reconstructed summer temperatures of <math>9-11^{\circ}\text{C}</math> (Bolland et al., 2021; Walkling, 1997) for  
1053 minor interstadial phases such as in Li-I or in Salzgitter-Lebenstedt (Pastoors, 2001) suggest  
1054 cold summers in tundra-like landscapes, forming a challenging environment for Neanderthals.  
1055 Further evidence of their successful adaptation to the cold climatic conditions of late MIS 5a,  
1056 the onset of MIS 4, and early MIS 3 in northern Central Europe also comes from a large number  
1057 of late Middle Paleolithic Keilmessergruppen sites and surface collections (Fig. 8a) that are  
1058 aggregated along the river valleys and associated with sediments mainly dating to early MIS 3  
1059 (Mol, 1995; Weiss, 2015; Weiss et al., 2018; Winsemann et al., 2015). These assemblages,  
1060 although only typologically attributed to the Keilmessergruppen, show that Lichtenberg is not  
1061 the northernmost limit of the Neanderthal habitat (Nielsen et al., 2017), as late Middle  
1062 Paleolithic sites, such as Ochtmissen (Thieme, 2003), Lower Saxony/ Germany and Dreisdorf  
1063 (Hartz et al., 2012), Schleswig-Holstein/ Germany are located even further north (Fig. 8a).

1064  
1065 Currently, we are missing direct evidence for Neanderthal occupations of northern Central  
1066 Europe during the peak of MIS 4. Whereas some authors suggest that Neanderthals migrated  
1067 south (Jöris, 2004) during that period, others even consider local extinctions of Neanderthal  
1068 groups (Hublin and Roebroeks, 2009). However, the Keilmesser tools show technological  
1069 continuity that connects MIS 5a with early MIS 3 assemblages (Fig. 8c). This is demonstrated

1070 in the assemblages of Königsau A and C (MIS 5a (Jöris, 2004; Mania, 2002; Mania and Toepfer,  
1071 1973)), Salzgitter-Lebenstedt (MIS 5a/4 or MIS 4/3 (Jöris, 2004; Pastoors, 2009, 2001)), and  
1072 Pouch, Saxony-Anhalt/ Germany (MIS 3 (Weiss, 2015; Weiss et al., 2018)), where the  
1073 Keilmesser share the main technological and morphological features with those from  
1074 Lichtenberg (Weiss, 2020) (Fig. 8c). Furthermore, some of the MIS 3 Keilmesser from the G-  
1075 Complex of the Sesselfelsgrötte (Richter, 2002, 1997) also show morpho-technological  
1076 similarities to those from Lichtenberg (Delpiano and Uthmeier, 2020), potentially indicating  
1077 seasonal, migrations to southern regions of Central Europe during the late Middle Paleolithic.  
1078 Altogether, the techno-typological continuity of late Neanderthal assemblages in northern  
1079 Central Europe between MIS 5a and MIS 3, as well as the successful adaptation to cold  
1080 environments, favor the hypothesis of seasonal migrations during cold periods instead of local  
1081 extinctions.

1082

1083 In summary, Li-I proves the presence of Neanderthals in the north during cold, stadial climatic  
1084 conditions. This assemblage represents a short-term butchering stay associated with the  
1085 central and eastern European Keilmessergruppen. We suggest that Neanderthals populated  
1086 the north intensively until early MIS 3, and adapted their life ways to the regional cold climatic  
1087 conditions.

1088

## 1089 **6. Conclusion**

1090 (1) In Lichtenberg, we have established a high-resolution chronological framework based  
1091 on the luminescence dating results as well as sedimentological, paleoenvironmental,  
1092 and archaeological analyses. This allowed us to connect the northern Neanderthal  
1093 occupations to climatically different phases of the last interglacial-glacial cycle, with a  
1094 chronological resolution close to the millennial scale of Greenland  
1095 Interstadials/Stadials (section 5.2).

1096 (2) The chronostratigraphic results led to a revision of the timing for the occupation Li-I in  
1097 Lichtenberg. We obtained consistent ages for this find layer with a mean of  
1098  $71.3 \pm 7.3$  ka replacing the former mean age of  $57 \pm 6$  ka, which was likely rejuvenated  
1099 by post-depositional cryoturbation. Our new age complies with the stratigraphic and  
1100 paleoenvironmental findings and is therefore considered robust and reliable.

- 1101 (3) By reporting the age for the occupation Li-II (mean of  $90.5 \pm 8.7$  ka), we also present  
1102 the first independent ages of the latest Brörup Interstadial WE IIb in its type region in  
1103 northern Central Europe. The age suggests that the terminations of the continental  
1104 Brörup and MIS 5c broadly coincide (section 5.1). This is valuable information for  
1105 numerous paleoenvironmental and archaeological sites in the area, where the  
1106 chronologies rely on biostratigraphical evidence alone.
- 1107 (4) The high-resolution chronological framework enabled us to show that Neanderthals  
1108 inhabited the northern regions of central Europe during the Eemian, the early last  
1109 glacial interstadials, as well as during the onset of the first glacial maximum. We  
1110 conclude, they lived in changing environments: a wooded landscape during the Eemian  
1111 pollen zone E IVb/V, a boreal landscape opening up during late MIS 5c and a dry tundra-  
1112 like environment during earliest MIS 4.
- 1113 (5) The changing archaeological record tentatively implies resilient adaptations to  
1114 changing environments. These are inferred from different raw material availabilities  
1115 and resulting management strategies, as well as a high-typological tool diversity in Li-  
1116 II versus specialized cutting tools and a potentially highly-mobile tool kit in Li-I. This is  
1117 supported by the use-wear analysis that demonstrated a variety of tasks in Li-II in  
1118 contrast to potentially specialized cutting tasks in Li-I only. Furthermore, raw material  
1119 availability can also be explained by geomorphic factors. Sediment redeposition, which  
1120 provided high-quality and large flint raw material from the primary source of the glacial  
1121 sediments nearby was hindered in the forested intervals (Li-II and the Eemian  
1122 occupation) and fostered in the much more sparsely-vegetated phases (Li-I). Future  
1123 work is planned to evaluate our preliminary results.
- 1124 (6) Most importantly, we could show that Neanderthals occupied the northern regions of  
1125 central Europe also during the cold phases of the last Glacial (section 5.5). Similarities  
1126 in the archaeological record, especially the technological similarities of Keilmesser  
1127 manufacture (see above) between Li-I and the posterior early MIS 3 sites further  
1128 suggest the potential recurrence of populations in the region. That Neanderthals  
1129 successfully adapted to the harsh northern climatic conditions is corroborated by the  
1130 fact that early MIS 3 sites are by far the most numerous Middle Paleolithic sites in the  
1131 North.  
1132

Figures

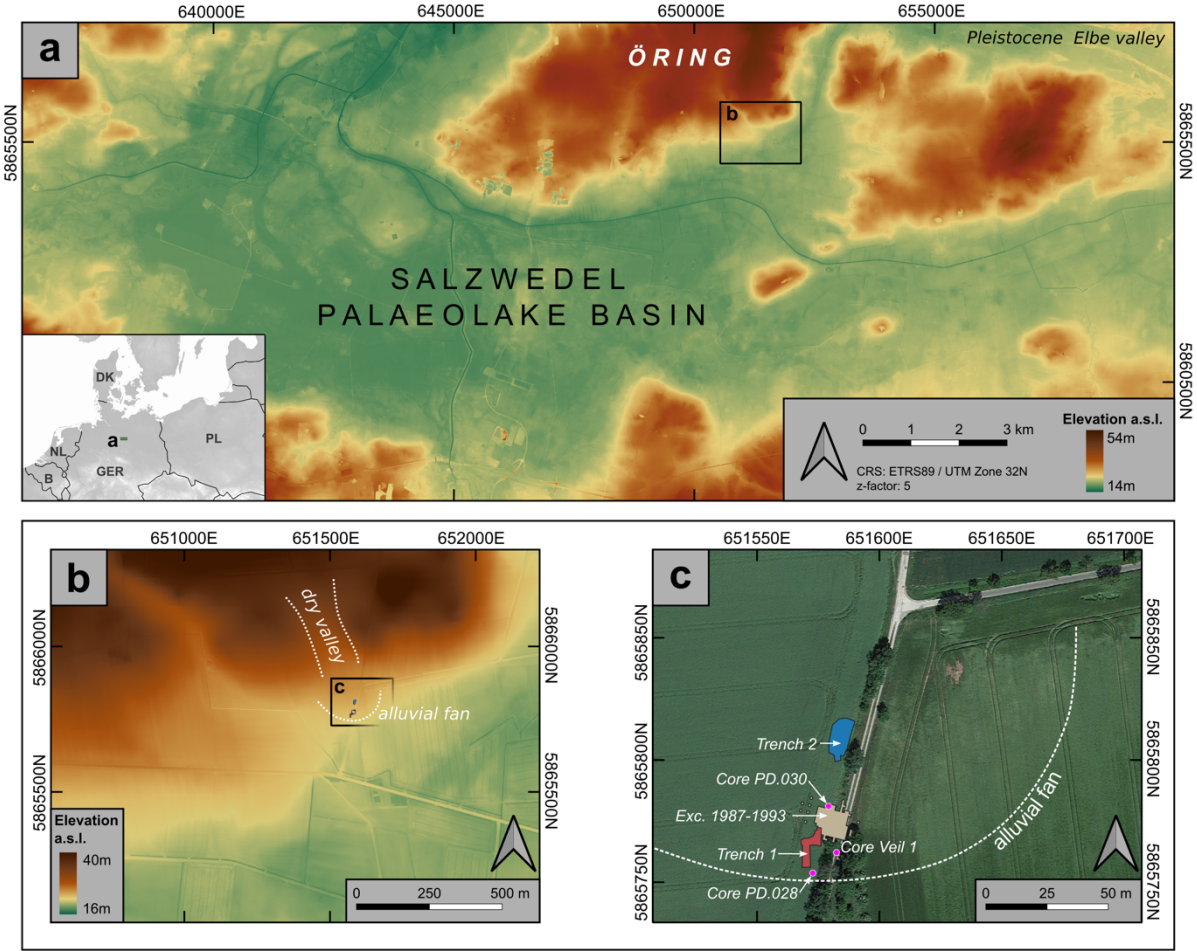


**Figure 1:** Location of the study area in Northern Germany (a). The sites are situated on a small alluvial fan surrounded by lowlands (b). Panel c indicates the position of the archaeological trenches 1 and 2, the previous excavation area (1987-1993) and three sediment cores mentioned in the text (PD.028, PD.030, Veil 1). Digital elevation model (DEM 1) provided by the State Offices for Geoinformation and Land Survey in Lower Saxony and Saxony-Anhalt.

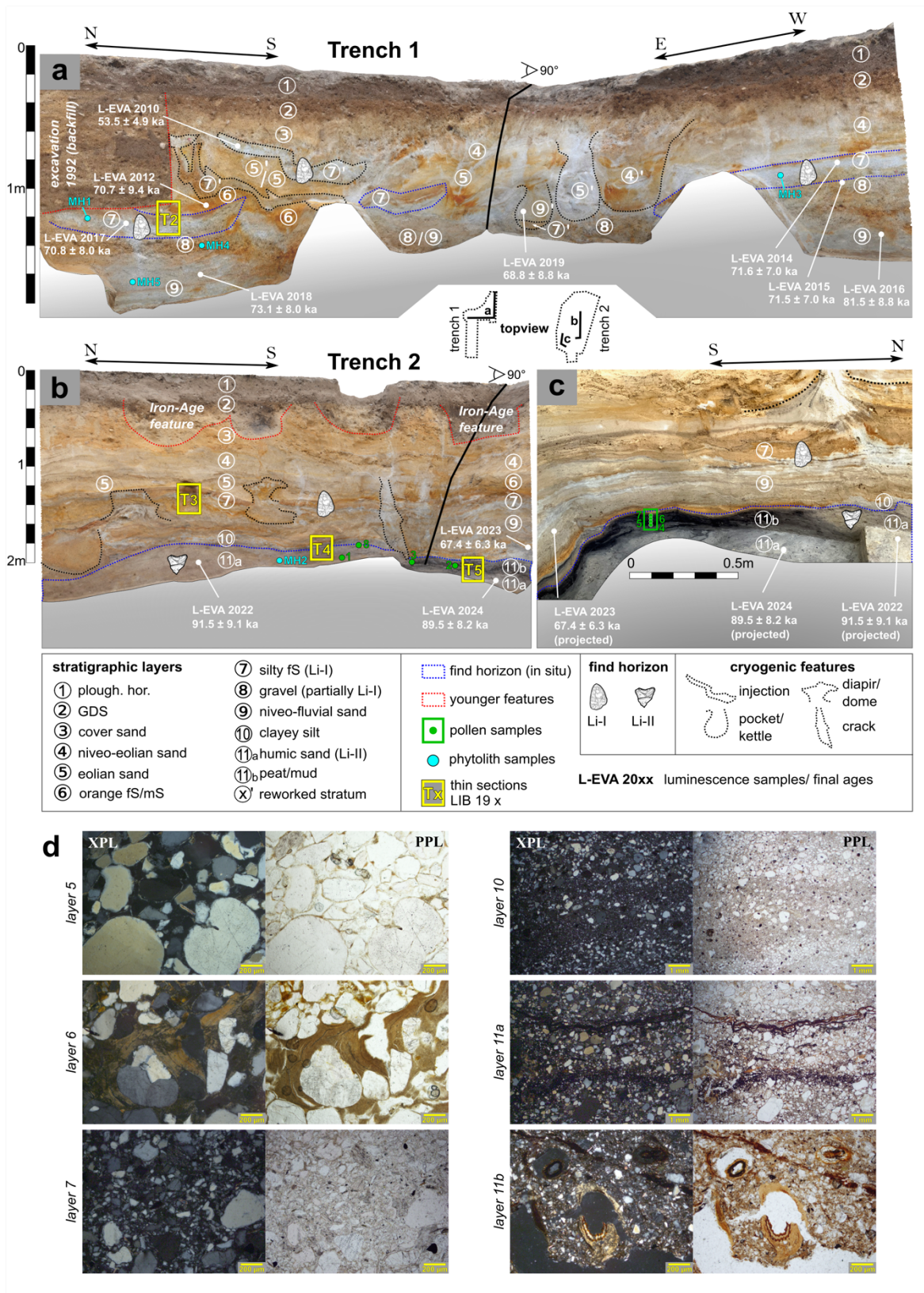


**Figure 2:** Stratigraphic features and archaeological horizons, along with sampling positions for luminescence dating, pollen analysis and micromorphology in Trench 1 (a) and Trench 2 (b and c). GDS refers to “Geschiebedecksand” a late Weichselian solifluction layer (Tab. 1, Supplementary Section 5.1). (d) Microphotographs of thin sections in cross-polarized (XPL) and plane-polarized (PPL) light. Photograph of layer 5 taken from sample T3, layer 6 from T1,

layer 7 from T2, layers 10 and 11a from T4 and layer 11b from T5. Layer 5 is dominantly composed of coarse sand to silty quartz grains in a massive microstructure; layer 5 shows the same composition as layer 6, but here void space is filled by clay illuviation; layer 7 shows a poor sorting for fine sand to silt sized quartz grains in a dense microstructure that presents a barrier for the clay moving down with pore water; layer 10 shows bedding of silty to coarse-sand sized quartz; layer 11a is characterized by organic-rich bands composed of amorphous staining, plant cells and tissues with rare bioturbation voids; in layer 11b organic residues increase in size as well as number and bioturbation voids are more ubiquitous.

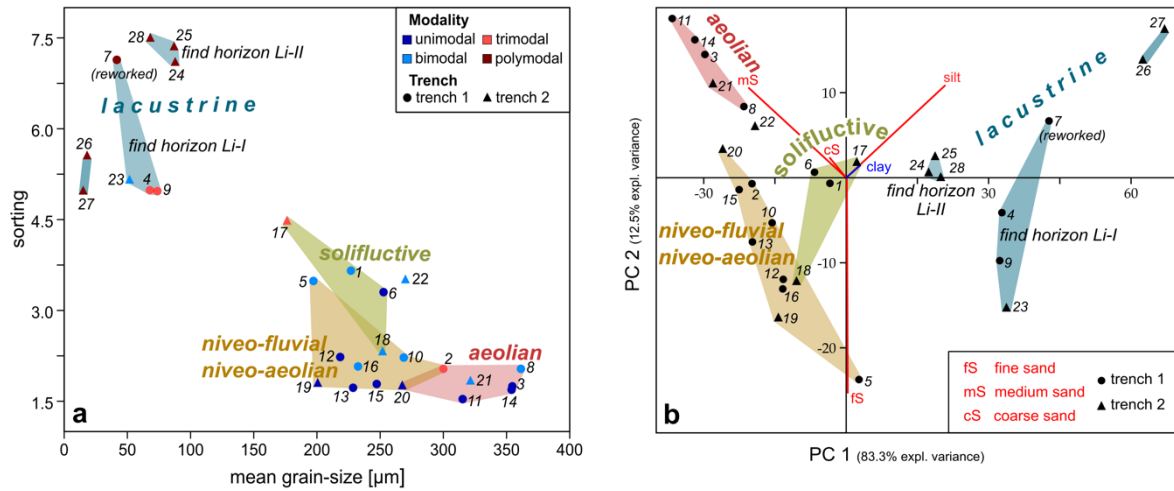


**Figure 3:** Statistical analyses of grain size results. (a) Scatter plot of sorting and mean grain size. (b) Principle component analysis (PCA) with the most significant principle components (PC1 and PC2) shown. Convex hulls of sedimentary processes according to classification during field description. Stratigraphic layers related to the sample codes indicated in Tab. 1.

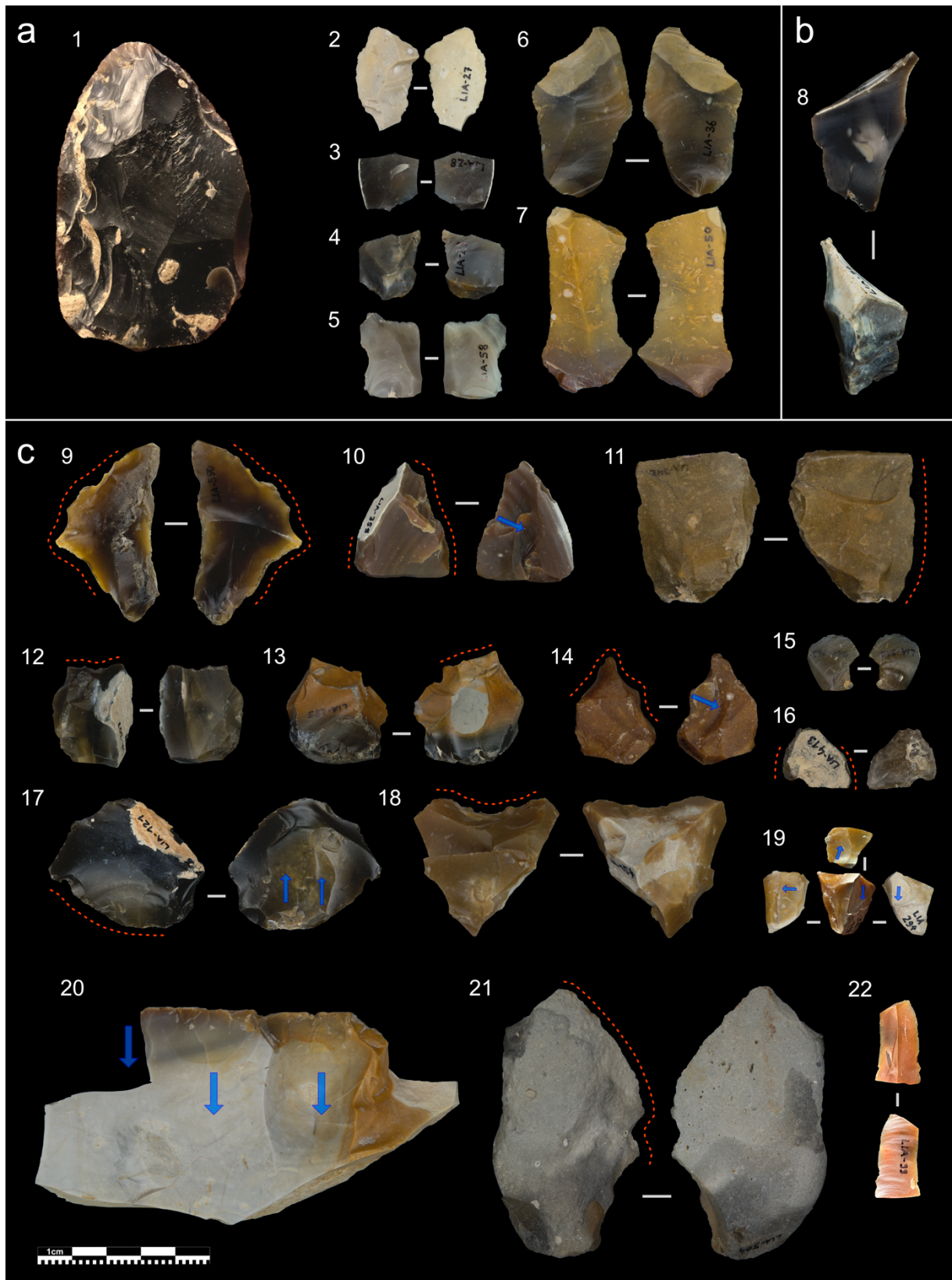


**Figure 4:** Artefacts from Lichtenberg I (a), (b) and II (c) discovered in Trench 1 (a) and Trench 2 (b), (c). (a) 1 – Keilmesser (Li-7; Layer 7’); 2 – flake (LIA-27; Layer 7); 3 – proximal flake (LIA-28; Layer 7); 4 – flake (LIA-29; Layer 7); 5 – flake (LIA-58; Layer 8); 6 – flake from bifacial tool production (LIA-36; Layer 7); 7 – flake (LIA-50; Layer 8); (b) 8 – flake (LIA-74; Layer 7); (c) (all Layer 11a): 9 – flake with heavy macroscopic use-wear (LIA-550); 10 – scraper with ventral surface removal and thermal alteration (LIA-359); 11 – backed knife with macroscopic use-

wear (LIA-342); 12 – endscraper on thick flake (LIA-307); 13 – endscraper on thick flake (LIA-285); 14 – denticulate on thick flake with dorsal surface removal (LIA-377); 15 – small flake with fresh, sharp edged preservation (LIA-330); 16 – distal scraper fragment with thermal alteration (LIA-413); 17 – flake with macroscopic use-wear and with ventral surface removals (LIA-121); 18 – complex notch on core (LIA-154); 19 – small irregular core (LIA-294); 20 – large core on low quality raw material with internal cracks (LIA-335); 21 – flake tool with notch and sharp edge on large quartzite flake (LIA-504); 22 – medial blade fragment (LIA-99). Red dotted lines mark macroscopic working edges, blue arrows mark larger surface removals and removals on cores. Photos: MPI EVA.

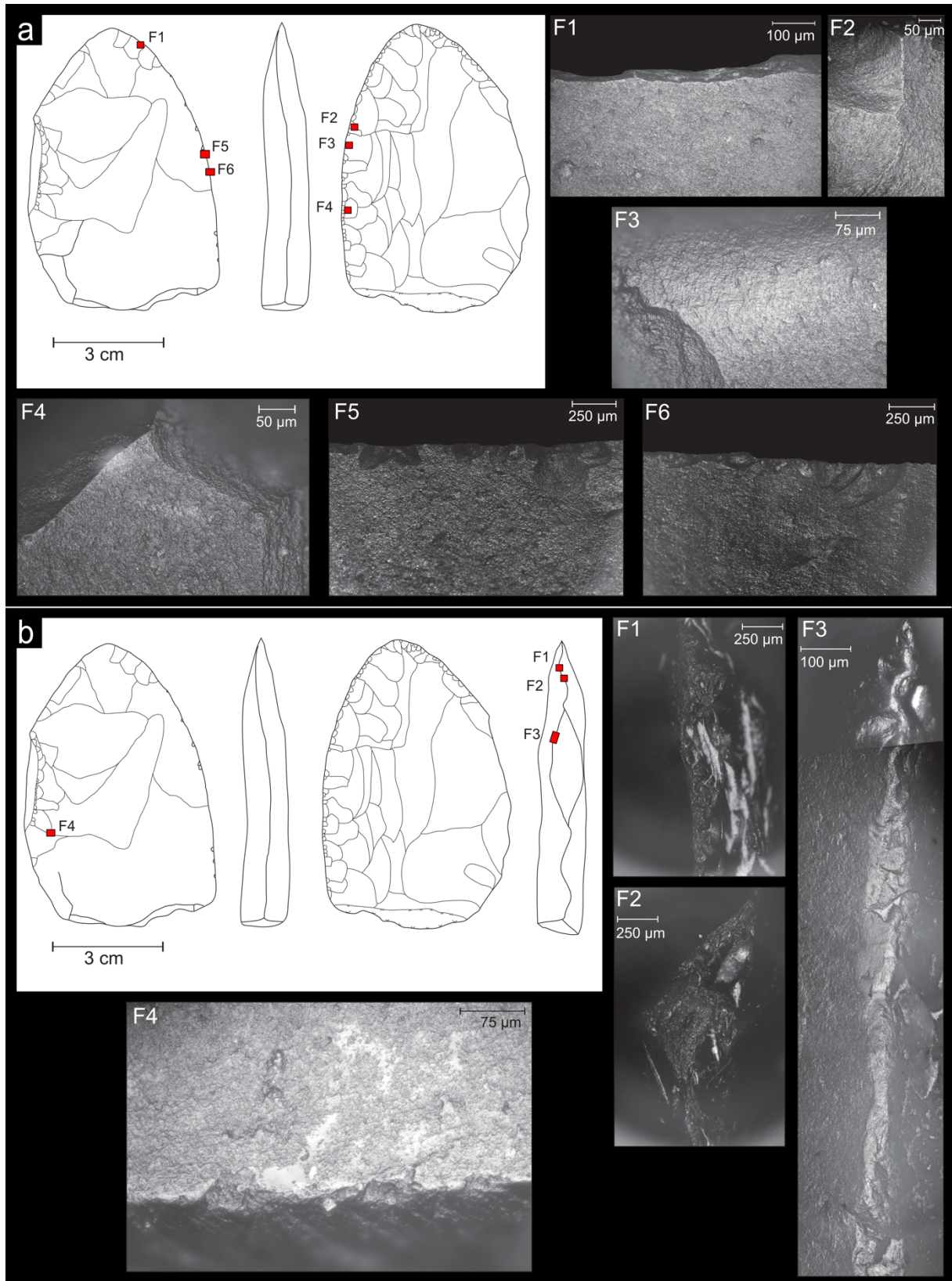


**Figure 5:** Results of the traceology for the Keilmesser Li-7. (a) Use-wear traces along the working edge. F1 - taken at magnification 200x, micrograph of the light developed bright polish on the edge of the active zone of the tool; F2 - taken at magnification 200x, micrograph showing the rounded and polished edges of the negatives on the dorsal surface of the working edge; F3 and F4 – both taken at magnification 200x, micrographs of the striations on the interior of the dorsal side of the tools' working edge; F5 and F6 – both taken at magnification

50x, micrographs of the micro-negatives on the ventral surface of the working edge. (b) Traces on the prehensile/hafting zone of the Keilmesser Li-7. F1 and F2 - both taken at magnification 50x, crushed and abraded edges on the back of the tool; F3 - taken at magnification 200x, composed micrograph images showing the undulating bright and well interconnected polish on the edge of the negative forming the back of the Keilmesser; F4 - taken at magnification 200x, bright undulating G type polish on the ventral surface of the tool. Drawings and photographs: Y. H. Hilbert.

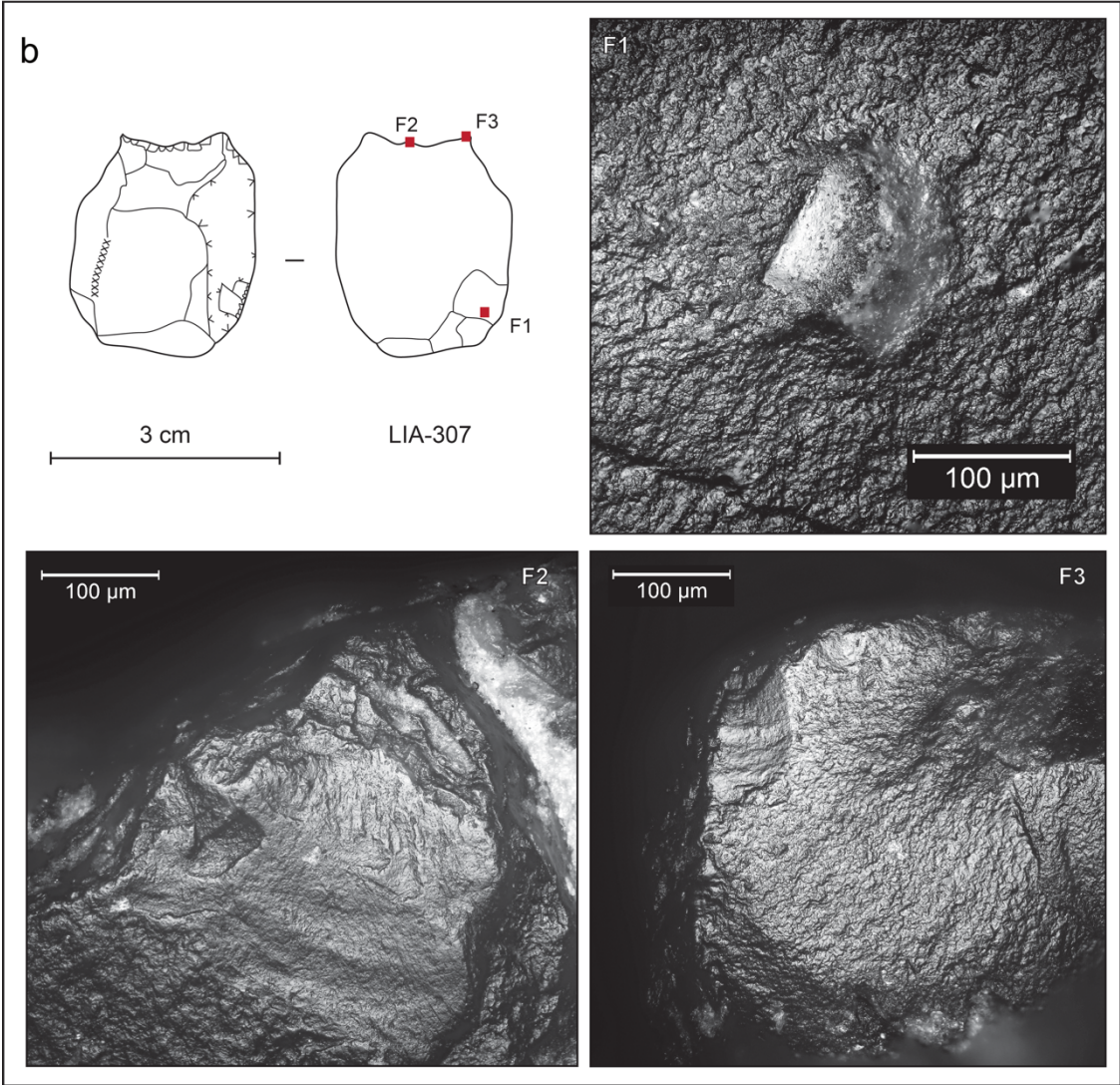
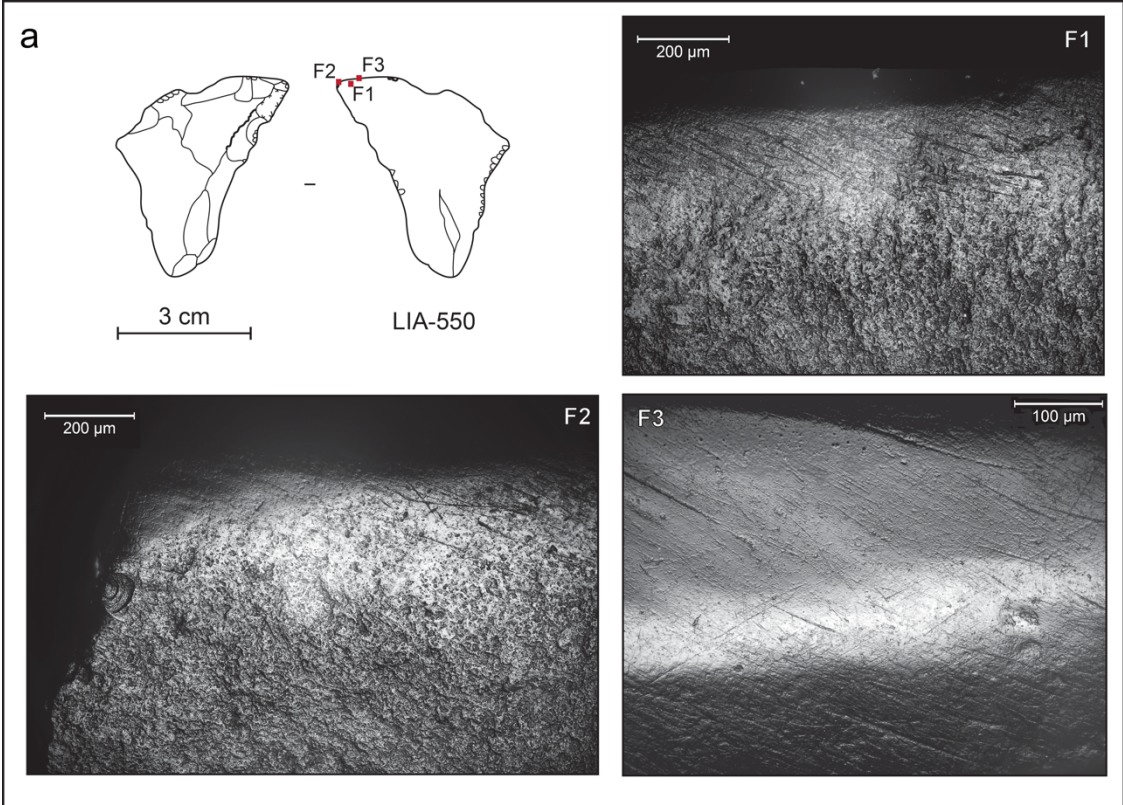


**Figure 6:** Results of the traceology for the Lichtenberg II assemblage. (a) Schema of artefact LIA-550 and the location of the micrographs showing the use related polish. F1 – taken at magnification 100x, bright undulating extensive polish located on the distal portion of the working edge; F2 – taken at magnification 100x on the edge of the working surface showing the spread of the bright undulating extensive polish, note the high incidence of striations and scratches; F3 – taken at magnification 200x at the center of the maximum extension of the micro polished surface on the working edge of the tool. The spread and connectedness of the polish is very high and the surface is extremely smoothed, again the criss-cross patterned motion of tool use is particularly evident by the striations and scratches. The resemblance to cereal polish is remarkable. Worked material: soft vegetal/ hard organic. (b) Schema of artefact LIA-307 and the location of the micrographs showing use and hafting related polish. F1 – flat bright polish located on the eminence of the micro topography on the ventral surface of the tool; F2 and F3 – negative edge rounding and bright undulating extensive polish on concave working surface. All micrographs taken at 200x. Worked material: hard organic/ wood. Drawings and photographs: Y. H. Hilbert.

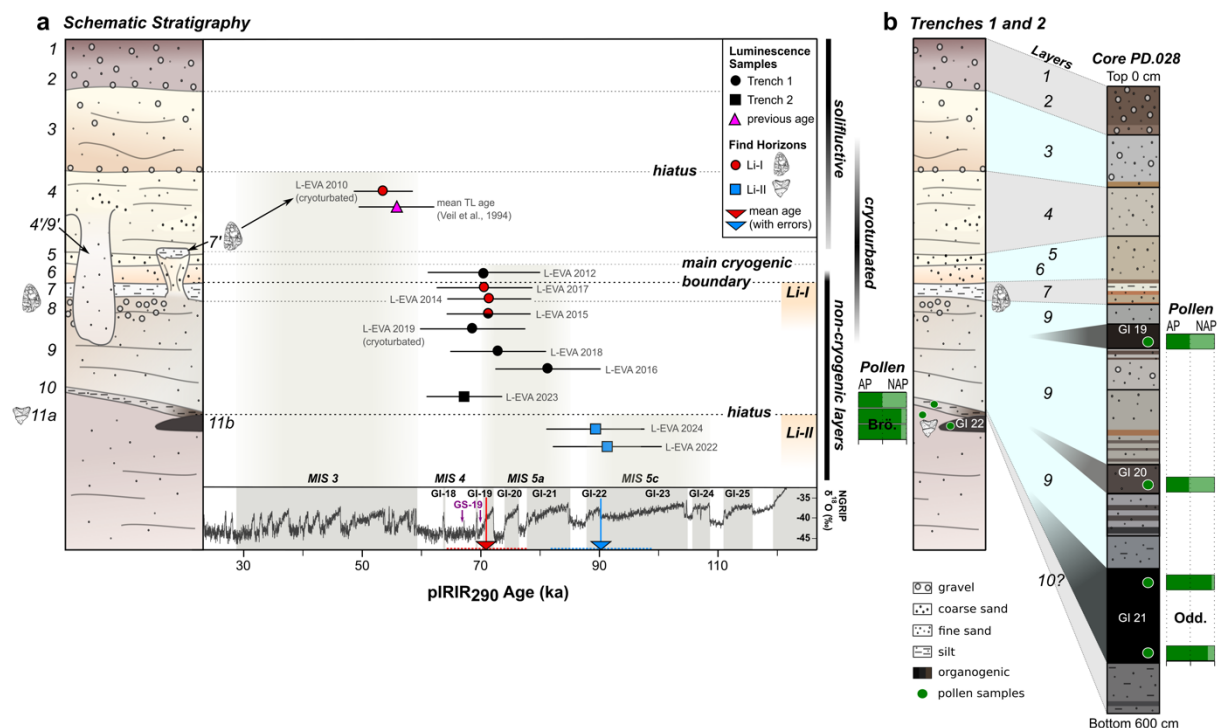


**Figure 7:** (a) Schematic stratigraphic column of Trenches 1 and 2 and luminescence dating results ( $1\sigma$  error); position of the find horizon is highlighted and indicated by a representative artefact symbol. On the x-axis, the time line and the NGRIP  $\delta^{18}O$  Greenland temperature proxy is provided (NGRIP Members, 2004). (b) Correlation of the schematic stratigraphy of the trenches with sediment core PD.028 (location in Fig. 1) and simplified results of palynological analysis. AP = arboreal pollen, NAP = non-arboreal pollen.

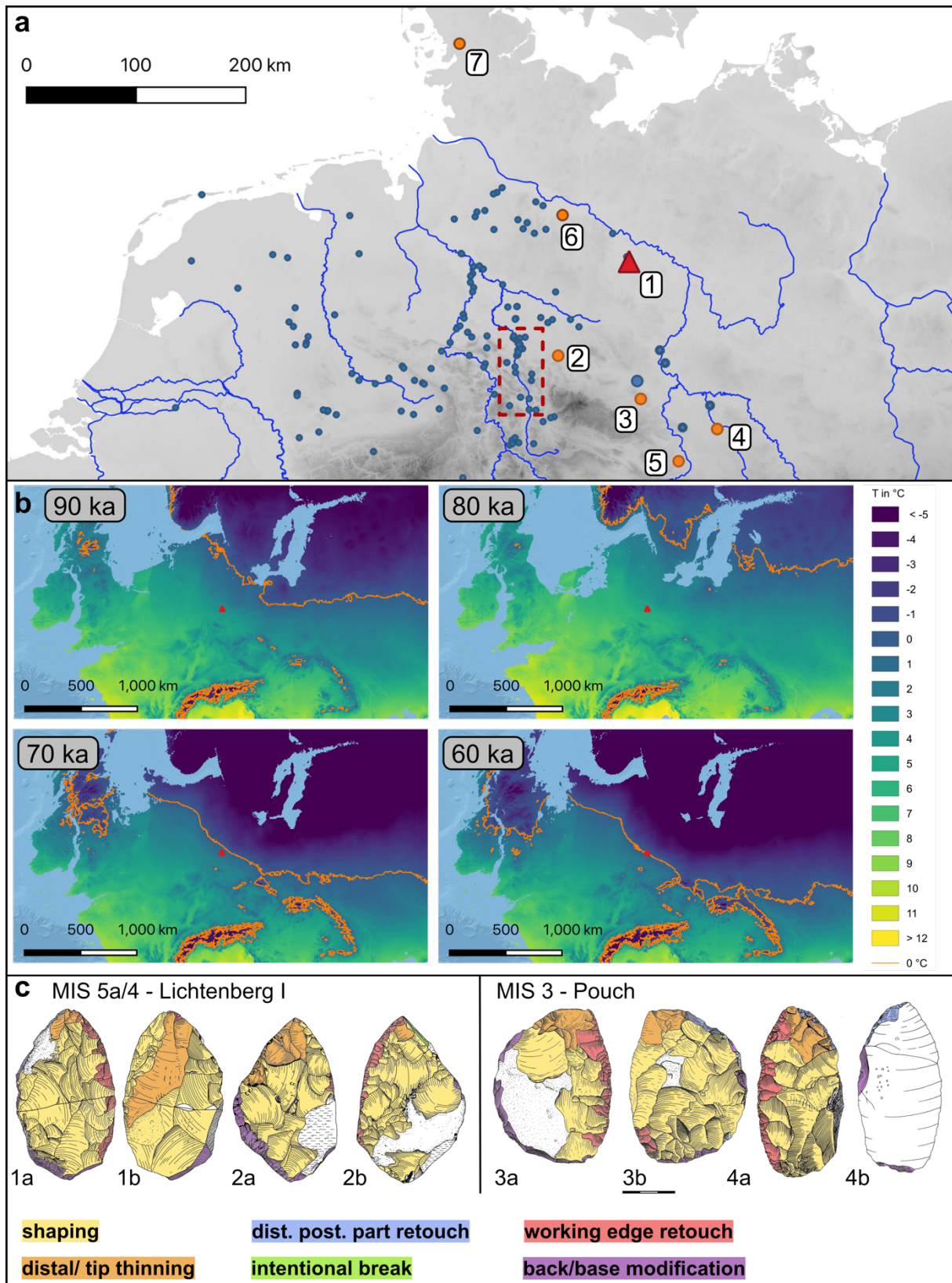


**Figure 8:** Distribution of late Middle Paleolithic sites in the study area (a), mean annual temperature change between 90 ka and 60 ka (b), and Keilmesser technology (c). (a) Displayed are the late Middle Paleolithic sites documented in the database of the State Service for Cultural Heritage Lower Saxony, Hannover, Germany. Most of them are surface collections. To make sure that they date between MIS 5a and MIS 3, only collections that include Keilmesser, Handaxes, and sometimes leafpoints as late Middle Paleolithic type

fossils were selected. Sites located in the rectangle were collected from a river terrace of the Leine Valley that was dated to early MIS 3 (Winsemann et al., 2015). 1 – 6 are sites mentioned in the text: 1 – Lichtenberg; 2 – Salzgitter-Lebenstedt; 3 – Königsau; 4 – Pouch; 5 – Neumark-Nord; 6 – Ochtmissen; 7 – Dreisdorf. The map is based on SRTM data V4 (<http://srtm.csi.cgiar.org>) (Jarvis et al., 2008; Reuter et al., 2007) and was generated in QGIS v3.12. (b) Change of the mean annual temperature with focus on northern central Europe. Red triangle: Lichtenberg; orange line: 0 °C isotherm. The map was created with the oscillayers dataset (<https://doi.org/10.5061/dryad.27f8s90>) (Gamisch, 2019a, 2019b) and generated in QGIS v3.12. (c) Technological comparison of Keilmesser from the MIS 5a/4 transition (Lichtenberg) and early MIS 3 (Pouch). The Keilmesser from both sites can be classified as type Lichtenberg. They show the same shaping technology, and moreover the Keilmesser from both sites are highly comparable regarding overall morphology, working edge morphology and treatment, as well as edge angle configurations (Weiss, 2020).

Layer	Pre- sence	Thickn. (cm)	Sediment Description	Interpretation	Grain Size Sample
1	Tr1, Tr2	< 40	Gravelly, slightly silty sand; very poorly sorted; humic (ca. 2%), related to layer 2	<b>ploughing horizon</b> formed in layer 2	–
2	Tr1, Tr2	< 25	Gravelly, slightly silty sand; very poorly sorted; coincides with brunified horizon (Cambisol); unbedded; higher gravel content than in layer 3	periglacial cover bed, ‘Geschiebedecksand’ ( <b>GDS</b> )	1, 17
3	Tr1, Tr2	50	Slightly gravelly and silty, poorly sorted, yellow medium sand; weakly-bedded; stoneline at its lower boundary	<b>cover sand</b> , solifluctive/colluvial facies	6, 18
4	Tr1, Tr2	50	Thin-bedded, wavy, moderately to poorly sorted, fine to medium sands; pale yellow; interbedded with thicker lenses of better sorted (aeolian) medium sands which are similar to layer 5	<b>niveofluvial to niveo-aeolian</b> facies, partially reworking layer 5 (?)	2, 19, 20,
4'	Tr1	pocket	Original structure of layer 4 recognisable, but deformed and slightly mixed within a pocket (ca. 50 cm deep); hydromorphic overprint	<b>cryoturbation pocket</b> affecting layer 4	13, 15
5	Tr1, Tr2	10/30	Very loose, yellow medium sand, better sorted than surrounding layers; inclined bedding to sheet-like (unbedded)	<b>aeolian sand</b> (saltation)	3, 8, 11, 21
5'	Tr1 (Tr2)	various	Similar characteristics as layer 5 but with cryogenic overprint (injections or pockets)	<b>cryoturbation</b> affecting layer 5	14
6	Tr1, Tr2	20	Poorly to moderately sorted, fine to medium sands, orange oxidation color; unbedded	no interpretation (may belong to adjacent layers)	22
7 Li-I	Tr1, Tr2	< 15	Fine sandy very coarse silt to silty very fine sands; whitish, brown-orange ferrugination on top with drop-shaped boundary on mm to cm-scale; very poorly sorted; contains <b>find horizon Li-I</b>	lacustrine <b>shoreline facies</b>	4, 9, 23
7' Li-I	Tr1 (Tr2)	10/20	Main characteristics similar to layer 7; distorted; mixing with medium sand; contains artefacts of <b>find horizon Li-I</b>	layer 7 injected upwards by <b>cryoturbation</b>	7
8	Tr1	20/40	Fine to medium gravelly, medium sands; poorly sorted; gleyic (greyish-light br.), crudely bedded, contains lithic artefacts in the upper 5 cm ( <b>lower part of find horizon Li-I</b> )	higher-energy <b>niveofluvial slopewash</b>	–
9	Tr1, Tr2	40/> 100	Thin-bedded, wavy, moderately to poorly sorted fine to medium sands; gleyic (greyish-light brown)	<b>niveofluvial slopewash</b>	5, 10, 12
9'	Tr1	pocket	Gleyic, poorly sorted fine sand, characteristics of layer 9 discernable, even weak wavy bedding	<b>cryoturbation pocket</b> affecting layer 9	16
10	Tr2	< 10	Gleyic, fine sandy to loamy silt; covers layer 11b as a thin veneer; contains very thin humic bed (drift line)	<b>lacustrine facies</b> , with contained <b>drift line</b>	26, 27, (28)
11a Li-II	Tr2	> 100	Very coarse-silty fine sand, slightly humic (<0.5%); very poorly sorted; unbedded; contains <b>find horizon Li-II</b> and abundant small pieces of charred organic matter (both esp. in the uppermost 11 cm)	<b>colluvial to lacustrine shoreline/beach</b> facies, contains drift lines	24, 25, (28)
11b (Li-II)	Tr2	< 20	Peaty organic mud, interfingering with layer 11a, contains some artefacts at the lower boundary ( <b>find horizon Li-II</b> ); in places overlain by thin (<1 cm) grey silt (part of layer 10?)	lake moor near the shoreline	–

**Table 1:** Sedimentary properties of the stratigraphic layers, including their interpretation (cf. Supplementary Section 5) and the sample codes for grain size analysis. Grain size samples taken layer-wise: samples 1-16 from Trench 1, samples 17 to 28 from Trench 2. The column “presence” indicates in which trench the respective layer occurs, Trench 1, Trench 2 or both (Tr1, Tr2).

Lab.-ID (L-EVA)	Layer	D <sub>e</sub> (Gy), 1σ	DR <sub>total</sub> (Gy/ka)	Age (ka), 1σ	OD (%)	No. al.	Dose Model <sup>1</sup>
2010	7'– Li-I	131.9 ± 4.3	2.46 ± 0.21	53.5 ± 4.9	14.7 ± 0.4	24	MAM
2012	6	110.7 ± 4.3	1.57 ± 0.20	70.7 ± 9.4	16.0 ± 0.5	24	MAM
2014	7 – Li-I	160.8 ± 3.8	2.25 ± 0.21	71.6 ± 7.0	11.3 ± 0.4	23	MAM
2015	8 – Li-I	174.8 ± 7.5	2.44 ± 0.21	71.5 ± 7.0	19.4 ± 0.6	24	CAM
2016	9	163.3 ± 5.0	2.00 ± 0.21	81.5 ± 8.8	11.8 ± 0.5	17	MAM
2017	7 – Li-I	143.9 ± 8.2	2.03 ± 0.20	70.8 ± 8.0	21.4 ± 0.6	24	MAM
2018	9	137.3 ± 3.4	1.88 ± 0.20	73.1 ± 8.0	11.7 ± 0.4	24	CAM
2019	9'	112.4 ± 3.4	1.63 ± 0.20	68.8 ± 8.8	13.9 ± 0.4	24	CAM
2022	11 – Li-	254.7 ± 16.7	2.78 ± 0.21	91.5 ± 9.1	29.4 ± 1.0	21	CAM
2023	9	155.0 ± 4.8	2.30 ± 0.20	67.4 ± 6.3	14.7 ± 0.5	24	CAM
2024	11 – Li-	241.1 ± 12.7	2.69 ± 0.20	89.5 ± 8.2	20.9 ± 0.7	22	WM

**Table 2:** Results of the De-measurements along with the final pIRIR<sub>290</sub> luminescence ages. OD = Overdispersion value. No.al = Number of aliquots included in the age calculations. CAM = Central Age Model, MAM = Minimum Age Model, WM = Weighted Mean. <sup>1</sup>σb value of 0.11 was used for MAM. The choice of age model is explained in Supplementary Section 6.3

Trench 2, excavation 2019		Trench 2, excavation 2020		Core PD.028		Biostratigraphy	MIS
Layer (Sample)	Vegetation	Layer (Sample)	Vegetation	Layer (Sample)	Vegetation		
n.r.	-	n.r.	-	peaty mud (12)	open landscape with dominant NAP (Poacea and heliophile herbs), <i>Pediastrum</i>	two minor interstadial oscillations in the earliest Schalkholz (WP I)	4
n.r.	-	n.r.	-	hum. sand (11)			
n.r.	-	n.r.	-	Peat (9, 10)	dense boreal forest with <i>Pinus</i> , <i>Betula</i> , <i>Juniperus</i> and <i>Larix</i>	Late Odderade Interstadial WE IV b	5a
10 (8)	<i>Betula</i> , very few <i>Pinus</i> , Poaceae, heliophyte-rich open vegetation, micro-charcoal peak	11b (7)	<i>Betula</i> , very few <i>Pinus</i> , Poaceae, heliophyte-rich ( <i>Ophioglossum</i> ) open vegetation, micro-charcoal peak	n.r.	-	Early Rederstall Stadial WE III	5b
n.r.	n.r.	11b (6) 11b (5)	Decrease of <i>Pinus</i> , increase of <i>Betula</i> and heliophytes	n.r.	-	Transition of WE II b to WE III	5c/5b
11b <sub>2</sub> (3) 11b (2) 11a (1)	Boreal forest opening up; <i>Pinus</i> , <i>Betula</i> , <i>Juniperus</i> , very few <i>Picea</i> , <i>Alnus</i> and <i>Larix</i> ; Poaceae; <i>Selaginella</i> <i>selaginoides</i> , <i>Ophioglossum</i> , <i>Botrychium</i>	11b (4)	Boreal forest opening up; <i>Pinus</i> , <i>Betula</i> , <i>Juniperus</i> , very few <i>Picea</i> , <i>Alnus</i> and <i>Larix</i> ; Poaceae; <i>Selaginella</i> <i>selaginoides</i> , <i>Ophioglossum</i> , <i>Botrychium</i>	n.r.	-	Late Brörup Interstadial WE II b  find horizon Li-II	MIS 5c

**Table 3:** Comparison and correlation of pollen samples 1 to 8, taken from layer 11 and 10, trench 2 (2019 and 2020 excavations) and samples 9 to 12 (core PD.028). Biostratigraphic assignment follows Menke and Tynni (1984); Behre and Lade (1986). For sampling codes and positions, see Fig 2b/c, Supplementary Figure S59. n.r. = not resolved. Correlation with Marine Isotope Stages (MIS) follows Lisiecki and Raymo (2005) and the lithostratigraphic

lexicon LITHOLEX of the German Federal Institute for Geosciences and Natural Resources, BGR (<https://litholex.bgr.de>).

<b>tool type</b>	<b>number</b>	<b>percent</b>	<b>example</b>
backed knife	1	2%	Fig. 4: 11
denticulate	3	6.3%	Fig. 4: 14
(limited) edge retouch	8	16.7%	Supplementary Figure S39
endscraper	8	16.7%	Fig. 4: 12, 13
endscraper, reused as hammerstone	1	2%	-
endscraper-scrapers	1	2%	-
hammerstone	3	6.3%	Supplementary Figure S38
naturally backed knife	1	2%	Supplementary Figure S40
notch	11	22.9%	Fig. 4: 18, 21
scrapers	2	4.2%	Fig. 4: 10, 16
flakes with possible use-wear	9	18.8%	Fig. 4: 9, 17
not identifiable	1	-	-
<b>total</b>	<b>49</b>	<b>100%</b>	-

**Table 4:** Tool types Lichtenberg II.

## **Acknowledgements**

We would like to thank Jonathan Schultz for geodata management and cartographic support, Sonja Riemenschneider for performing grain size analysis and Steffi Hesse and Victoria Krippner for luminescence sample preparation. For assistance during field work, we are grateful to Shannon P. McPherron, Nicolas Bourgon, Sarah Pederzani, Sabine Dietel, Marie Kaniecki, Felix Riedel, Jonathan Schultz, Wiebke E. Lüdtkke, Lia Berani, Floriske Meindersma, Annika Wiebers, Detlef Trapp and Mario Pahlow. We thank Family Kusserow in Lichtenberg who granted access to their land. The authors thankfully acknowledge the work done by the QSR editors and two anonymous reviewers who helped to improve the manuscript. For financial funding we owe our gratitude to Jean-Jacques Hublin (MPI EVA) and the Max Planck Society (MPG).

## References

- AG Boden, 2005. *Bodenkundliche Kartieranleitung KA5*, 5. Aufl. ed. Ad-hoc-Arbeitsgruppe Boden.
- Aiello, L.C., Wheeler, P., 2003. Neanderthal Thermoregulation and the Glacial Climate, in: van Andel, T.H., Davies, W. (Eds.), *Neanderthals and Modern Humans in the European Landscape during the Last Glaciation*. McDonald Institute for Archaeological Research, Cambridge, pp. 147–166.
- Aitken, M.J., 1998. *An introduction to optical dating: the dating of Quaternary sediments by the use of photon-stimulated luminescence*. Oxford University Press, New York.
- Antoine, P., Coutard, S., Guerin, G., Deschodt, L., Goval, E., Loch, J.-L., Paris, C., 2016. Upper Pleistocene loess-palaeosol records from Northern France in the European context: Environmental background and dating of the Middle Palaeolithic. *Quaternary International* 411, 4–24. <https://doi.org/10.1016/j.quaint.2015.11.036>
- Antoine, P., Rousseau, D.-D., Degeai, J.-P., Moine, O., Lagroix, F., Kreuzer, S., Fuchs, M., Hatté, C., Gauthier, C., Svoboda, J., Lisá, L., 2013. High-resolution record of the environmental response to climatic variations during the Last Interglacial–Glacial cycle in Central Europe: the loess-palaeosol sequence of Dolní Věstonice (Czech Republic). *Quaternary Science Reviews* 67, 17–38. <https://doi.org/10.1016/j.quascirev.2013.01.014>
- Behre, K.-E., 1989. Biostratigraphy of the last glacial period in Europe. *Quaternary Science Reviews* 8, 25–44. [https://doi.org/10.1016/0277-3791\(89\)90019-X](https://doi.org/10.1016/0277-3791(89)90019-X)
- Behre, K.-E., Hölzer, A., Lemdahl, G., 2005. Botanical macro-remains and insects from the Eemian and Weichselian site of Oerel (northwest Germany) and their evidence for the history of climate. *Vegetation History and Archaeobotany* 14, 31–53. <https://doi.org/10.1007/s00334-005-0059-x>
- Behre, K.-E., Lade, U., 1986. Eine Folge von Eem und 4 Weichsel-Interstadialen in Oerel/Niedersachsen und ihr Vegetationsablauf. *E&G Quaternary Science Journal* 36, 11–36. <https://doi.org/10.3285/eg.36.1.02>
- Behre, K.-E., van der Plicht, J., 1992. Towards an absolute chronology for the last glacial period in Europe: radiocarbon dates from Oerel, northern Germany. *Vegetation History and Archaeobotany* 1, 111–117. <https://doi.org/10.1007/BF00206091>
- Bertran, P., Andrieux, E., Antoine, P., Coutard, S., Deschodt, L., Gardère, P., Hernandez, M., Legentil, C., Lenoble, A., Liard, M., Mercier, N., Moine, O., Sitzia, L., Van Vliet-Lanoë, B., 2014. Distribution and chronology of Pleistocene permafrost features in France: Database and first results. *Boreas* 43, 699–711. <https://doi.org/10.1111/bor.12025>
- Beug, H.-J., 2004. Leitfaden der Pollenbestimmung für Mitteleuropa und angrenzende Gebiete. *Germania* 87, 542.
- Beuselinck, L., Govers, G., Poesen, J., Degraer, G., Froyen, L., 1998. Grain-size analysis by laser diffractometry: comparison with the sieve-pipette method. *CATENA* 32, 193–208. [https://doi.org/10.1016/S0341-8162\(98\)00051-4](https://doi.org/10.1016/S0341-8162(98)00051-4)
- Blott, S.J., Pye, K., 2001. GRADISTAT: a grain size distribution and statistics package for the analysis of unconsolidated sediments. *Earth Surface Processes and Landforms* 26, 1237–1248. <https://doi.org/10.1002/esp.261>
- Boch, R., Cheng, H., Spötl, C., Edwards, R.L., Wang, X., Häuselmann, Ph., 2011. NALPS: a precisely dated European climate record 120–60 ka. *Climate of the Past* 7, 1247–1259. <https://doi.org/10.5194/cp-7-1247-2011>
- Bolland, A., Kern, O.A., Allstädt, F.J., Peteet, D., Koutsodendris, A., Pross, J., Heiri, O., 2021. Summer temperatures during the last glaciation (MIS 5c to MIS 3) inferred from a

- 50,000-year chironomid record from Füramoos, southern Germany. *Quaternary Science Reviews* 264, 107008. <https://doi.org/10.1016/j.quascirev.2021.107008>
- Bordes, F., 1961. *Typologie du Paléolithique ancien et moyen*, Mémoires de l'Institut Préhistoriques de l'Université de Bordeaux. Delmas, Bordeaux.
- Bos, J.A.A., Bohncke, S.J.P., Kasse, C., Vandenberghe, J., 2001. Vegetation and climate during the Weichselian Early Glacial and Pleniglacial in the Niederlausitz, eastern Germany ? macrofossil and pollen evidence. *Journal of Quaternary Science* 16, 269–289. <https://doi.org/10.1002/jqs.606>
- Bosinski, G., 1967. *Die Mittelpaläolithischen Funde im Westlichen Mitteleuropa*. Fundamenta A/4. Böhlau-Verlag, Köln, Graz.
- Bouma, J., Foc, C.A., Miedma, R., 1990. Micromorphology of Hydromorphic Soils: Applications for Soil Genesis and Land Evaluation, in: Douglas, L.A. (Ed.), *Soil Micro-Morphology: A Basic and Applied Science*. pp. 257–278.
- Bridge, J., Demicco, R., 2008. *Earth Surface Processes, Landforms and Sediment Deposits*. Cambridge University Press, New York.
- Buylaert, J.P., Jain, M., Murray, A.S., Thomsen, K.J., Thiel, C., Sohbaty, R., 2012. A robust feldspar luminescence dating method for Middle and Late Pleistocene sediments. *Boreas* 41, 435–451. <https://doi.org/10.1111/j.1502-3885.2012.00248.x>
- Caspers, G., Freund, H., 2001. Vegetation and climate in the Early- and Pleni-Weichselian in northern Central Europe. *Journal of Quaternary Science* 16, 31–48. [https://doi.org/10.1002/1099-1417\(200101\)16:1<31::AID-JQS577>3.0.CO;2-3](https://doi.org/10.1002/1099-1417(200101)16:1<31::AID-JQS577>3.0.CO;2-3)
- Chan, B., Francisco Gibaja, J., García-Díaz, V., Hoggard, C.S., Mazzucco, N., Rowland, J.T., Van Gijn, A., 2020. Towards an understanding of retouch flakes: A use-wear blind test on knapped stone microdebitage. *PLOS ONE* 15, e0243101. <https://doi.org/10.1371/journal.pone.0243101>
- Christiansen, H.H., 1998a. Periglacial sediments in an Eemian-Weichselian succession at Emmerlev Klev, southwestern Jutland, Denmark. *Palaeogeography, Palaeoclimatology, Palaeoecology* 138, 245–258. [https://doi.org/10.1016/S0031-0182\(97\)00117-X](https://doi.org/10.1016/S0031-0182(97)00117-X)
- Christiansen, H.H., 1998b. Nivation forms and processes in unconsolidated sediments, NE Greenland. *Earth Surface Processes and Landforms* 23, 751–760. [https://doi.org/10.1002/\(SICI\)1096-9837\(199808\)23:8<751::AID-ESP886>3.0.CO;2-A](https://doi.org/10.1002/(SICI)1096-9837(199808)23:8<751::AID-ESP886>3.0.CO;2-A)
- Churchill, S.E., 2008. Bioenergetic perspectives on Neanderthal thermoregulatory and activity budgets, in: Harvati, K., Harrison, T. (Eds.), *Neanderthals Revisited: New Approaches and Perspectives*. Springer, pp. 113–134.
- Clemente, I., Gibaja, J.F., 1998. Working Processes on Cereals: An Approach Through Microwear Analysis. *Journal of Archaeological Science* 25, 457–464. <https://doi.org/10.1006/jasc.1997.0214>
- Cohen, A.S., 2003. *Paleolimnology: the history and evolution of lake systems*. Oxford University Press.
- Delpiano, D., Uthmeier, T., 2020. Techno-functional and 3D shape analysis applied for investigating the variability of backed tools in the Late Middle Paleolithic of Central Europe. *PLOS ONE* 15, e0236548. <https://doi.org/10.1371/journal.pone.0236548>
- Depaepe, P., Goval, É., Koehler, H., Locht, J.-L., 2015. Les plaines du Nord-Ouest : carrefour de l'Europe au Paléolithique moyen ?, *Mémoires de la société préhistorique française* 59. Société préhistorique française, Paris.
- Dibble, H.L., Sandgathe, D., Goldberg, P., McPherron, S., Aldeias, V., 2018. Were Western European Neanderthals Able to Make Fire? *Journal of Paleolithic Archaeology* 1, 54–79. <https://doi.org/10.1007/s41982-017-0002-6>

- Duphorn, K., Grube, F., Meyer, K.-D., Streif, H., Vinken, R., 1973. A. Area of Scandinavian Glaciation: 1. Pleistocene and Holocene. *E&G Quaternary Science Journal* 23/24, 222–250. <https://doi.org/10.3285/eg.23-24.1.19>
- Ehlers, J., 2020. *Das Eiszeitalter*. Springer Berlin Heidelberg, Berlin, Heidelberg. <https://doi.org/10.1007/978-3-662-60582-0>
- Ehlers, J., 1990. Untersuchungen zur Morphodynamik der Vereisungen Norddeutschlands unter Berücksichtigung benachbarter Gebiete. *Bremer Beiträge zur Geographie und Raumplanung* 19, 166.
- Ehlers, J., Grube, A., Stephan, H.J., Wansa, S., 2011. Pleistocene glaciations of North Germany-New results, *Developments in Quaternary Science*. <https://doi.org/10.1016/B978-0-444-53447-7.00013-1>
- Fægri, K., Iversen, J., Kaland, P.E., Krzywinski, K., 1989. *Textbook of pollen analysis*, 4th ed. John Wiley & Sons Ltd., Chichester.
- Farrell, E.J., Sherman, D.J., Ellis, J.T., Li, B., 2012. Vertical distribution of grain size for wind blown sand. *Aeolian Research* 7, 51–61. <https://doi.org/10.1016/j.aeolia.2012.03.003>
- Féblot-Augustins, J., 1993. Mobility Strategies in the Late Middle Palaeolithic of Central Europe and Western Europe: Elements of Stability and Variability. *Journal of Anthropological Archaeology*. <https://doi.org/10.1006/jaar.1993.1007>
- Folk, R.L., Ward, W.C., 1957. Brazos River bar [Texas]; a study in the significance of grain size parameters. *Journal of Sedimentary Research* 27, 3–26. <https://doi.org/10.1306/74D70646-2B21-11D7-8648000102C1865D>
- French, H., 2008. Recent contributions to the study of past permafrost. *Permafrost and Periglacial Processes* 19, 179–194. <https://doi.org/10.1002/ppp.614>
- Fuchs, M., Kreuzer, S., Rousseau, D.-D., Antoine, P., Hatté, C., Lagroix, F., Moine, O., Gauthier, C., Svoboda, J., Lisá, L., 2013. The loess sequence of Dolní Věstonice, Czech Republic: A new OSL-based chronology of the Last Climatic Cycle. *Boreas* 42, 664–677. <https://doi.org/10.1111/j.1502-3885.2012.00299.x>
- Gamisch, A., 2019a. Oscillayers: A dataset for the study of climatic oscillations over Plio-Pleistocene time scales at high spatial-temporal resolution. *Dryad, Dataset [WWW Document]*. <https://doi.org/https://doi.org/10.5061/dryad.27f8s90>
- Gamisch, A., 2019b. Oscillayers: A dataset for the study of climatic oscillations over Plio-Pleistocene time-scales at high spatial-temporal resolution. *Global Ecology and Biogeography* 28, 1552–1560. <https://doi.org/10.1111/geb.12979>
- Gaudzinski, S., 1999. Middle Palaeolithic Bone Tools from the Open-Air Site Salzgitter-Lebenstedt (Germany). *Journal of Archaeological Science* 26, 125–141. <https://doi.org/10.1006/jasc.1998.0311>
- Gaudzinski, S., 1998. Knochen und Knochengeräte der mittelpaläolithischen Fundstelle Salzgitter-Lebenstedt (Deutschland). *Jahrbuch des Römisch-Germanischen Zentralmuseums Mainz* 45, 163–220.
- Gaudzinski-Windheuser, S., Roebroeks, W., 2014. Multidisciplinary studies on the Middle Paleolithic record from Neumark-Nord (Germany). Volume I, *Veröffentlichungen des Landesamtes für Archäologie Sachsen-Anhalt* 69. Beier & Beran, Halle(Saale).
- Gladilin, V.N., 1976. *Problemy rannego paleolitha Vostocnoj Evropy*. Akademia nauk Ukrainskoj, SSR, Kiev.
- Glückler, R., Herzsuh, U., Kruse, S., Andreev, A., Vyse, S.A., Winkler, B., Biskaborn, B.K., Pestykova, L., Dietze, E., 2021. Wildfire history of the boreal forest of south-western Yakutia (Siberia) over the last two millennia documented by a lake-sediment charcoal record. *Biogeosciences* 18, 4185–4209. <https://doi.org/10.5194/bg-18-4185-2021>

- González-Urquijo, J.E., Ibañez-Estéves, J.J., 1994. Metodología de análisis funcional de instrumentos tallados en sílex. Universidad de Duesto.
- Grimm, E.C., 1990. TILIA, TILIAGRAPH and TILIAVIEW. PC spreadsheet and graphics software for pollen data.
- Grootes, P.M., 1978. Carbon-14 Time Scale Extended: Comparison of Chronologies. *Science* 200, 11–15. <https://doi.org/10.1126/science.200.4337.11>
- Hahne, J., Kemle, S., Merkt, J., Meyer, K.D., 1994. Eem-, weichsel- und saalezeitliche Ablagerungen der Bohrung “Quakenbrück GE 2.” *Geologisches Jahrbuch A134*, 9–69.
- Hartz, S., Beuker, J., Niekus, M.J.L.Th., 2012. Neanderthal finds in Schleswig Holstein? - Middle Palaeolithic flintscatters in Northern Germany, in: Niekus, M.J.L.Th., Barton, R.N.E., Street, M., Terberger, T. (Eds.), *A Mind Set on Flint. Studies in Honour of Dick Stapert*, Groningen Archaeological Studies 16. Barkhuis Groningen University Library, Groningen, pp. 93–105.
- Hedges, R.E.M., Pettitt, P.B., Ramsey, C.B., Klinken, G.J.V., 1998. Radiocarbon Dates from the Oxford AMS System: Archaeometry Datelist 25. *Archaeometry* 40, 227–239.
- Hein, M., Urban, B., Tanner, D.C., Buness, A.H., Tucci, M., Hoelzmann, P., Dietel, S., Kaniecki, M., Schultz, J., Kasper, T., Suchodoletz, H., Schwalb, A., Weiss, M., Lauer, T., 2021. Eemian landscape response to climatic shifts and evidence for northerly Neanderthal occupation at a palaeolake margin in northern Germany. *Earth Surface Processes and Landforms* esp.5219. <https://doi.org/10.1002/esp.5219>
- Hein, M., Weiss, M., Otcherednoy, A., Lauer, T., 2020. Luminescence chronology of the key-Middle Paleolithic site Khotylevo I (Western Russia) - Implications for the timing of occupation, site formation and landscape evolution. *Quaternary Science Advances* 2, 100008. <https://doi.org/10.1016/j.qsa.2020.100008>
- Hublin, J.-J., 1984. The fossil man from Salzgitter-Lebenstedt (FRG) and its place in human evolution during the Pleistocene in Europe. *Zeitschrift für Morphologie und Anthropologie* 75, 45–56.
- Hublin, J.-J., Roebroeks, W., 2009. Ebb and flow or regional extinctions? On the character of Neanderthal occupation of northern environments. *Comptes Rendus Palevol* 8, 503–509. <https://doi.org/10.1016/j.crpv.2009.04.001>
- Iovita, R., 2010. Comparing stone tool resharpening trajectories with the aid of elliptical Fourier analysis, in: Lycett, S.J., Chauhan, P.R. (Eds.), *New Perspectives on Old Stones. Analytical Approaches to Paleolithic Technologies*. Springer, pp. 235–253.
- Jarvis, A., Reuter, H.I., Nelson, A., Guevarra, E., 2008. Hole-filled seamless SRTM data V4, Centre for Tropical Agriculture (CIAT) [WWW Document]. URL <http://srtm.csi.cgiar.org>
- Jöris, O., 2012. Keilmesser, in: Floss, H. (Ed.), *Steinartefakte Vom Altpaläolithikum Bis in Die Neuzeit*. Kerns Verlag, Tübingen, pp. 297–308.
- Jöris, O., 2006. Bifacially backed knives (Keilmesser) in the central European Middle Palaeolithic, in: Goren-Inbar, N., Sharon, G. (Eds.), *Axe Age: Acheulian Tool-Making from Quarry to Discard*. Equinox Publishing Ltd, London, pp. 287–310.
- Jöris, O., 2004. Zur chronostratigraphischen Stellung der spätmittelpaläolithischen Keilmessergruppen: Der Versuch einer kulturgeographischen Abgrenzung einer mittelpaläolithischen Formengruppe in ihrem europäischen Kontext. *Bericht RGK* 84, 49–153.
- Katz, O., Cabanes, D., Weiner, S., Maeir, A.M., Boaretto, E., Shahack-Gross, R., 2010. Rapid phytolith extraction for analysis of phytolith concentrations and assemblages during an excavation: an application at Tell es-Safi/Gath, Israel. *Journal of Archaeological Science* 37, 1557–1563. <https://doi.org/10.1016/J.JAS.2010.01.016>

- Keeley, L.H., 1980. Experimental Determination of Stone Tool Uses: a Microwear Analysis. University of Chicago Press.
- Kegler, J.F., Fries, J.E., 2018. Neandertaler? 15m tiefer bitte! Die neandertalerzeitlichen Steinartefakte der Fundstellen Gildehaus 31 und 33 im Landkreis Graftschaft Bentheim (Niedersachsen). *Archäologisches Korrespondenzblatt* 48, 455–471.
- Kindler, L., Smith, G.M., García-Moreno, A., Gaudzinski-Windheuser, S., Pop, E., Roebroeks, W., 2020. The last interglacial (Eemian) lakeland of Neumark-Nord (Saxony-Anhalt, Germany). Sequencing Neanderthal occupations, assessing subsistence opportunities and prey selection based on estimations of ungulate carrying capacities, biomass production and energy, in: García-Moreno, A., Hutson, J.M., Smith, G.M., Kindler, L., Turner, E., Villaluenga, A., Gaudzinski-Windheuser, S. (Eds.), *Human Behavioural Adaptations to Interglacial Lakeshore Environments, RGZM - Tagungen 37*. RGZM, Mainz und Heidelberg, pp. 67–104.
- Kolobova, K.A., Roberts, R.G., Chabai, V.P., Jacobs, Z., Krajcarz, M.T., Shalagina, A. V., Krivosheina, A.I., Li, B., Uthmeier, T., Markin, S. V., Morley, M.W., O’Gorman, K., Rudaya, N.A., Talamo, S., Viola, B., Derevianko, A.P., 2020. Archaeological evidence for two separate dispersals of Neanderthals into southern Siberia. *Proceedings of the National Academy of Sciences* 117, 2879–2885.  
<https://doi.org/10.1073/pnas.1918047117>
- Kreutzer, S., Schmidt, C., Dewitt, R., Fuchs, M., 2014. The a-value of polymineral fine grain samples measured with the post-IR IRSL protocol. *Radiation Measurements* 69, 18–29.  
<https://doi.org/10.1016/j.radmeas.2014.04.027>
- Kühl, N., Litt, T., Schölzel, C., Hense, A., 2007. Eemian and Early Weichselian temperature and precipitation variability in northern Germany. *Quaternary Science Reviews* 26, 3311–3317. <https://doi.org/10.1016/j.quascirev.2007.10.004>
- Lambeck, K., 2004. Sea-level change through the last glacial cycle: geophysical, glaciological and palaeogeographic consequences. *Comptes Rendus Geoscience* 336, 677–689.  
<https://doi.org/10.1016/j.crte.2003.12.017>
- Lang, J., Lauer, T., Winsemann, J., 2018. New age constraints for the Saalian glaciation in northern central Europe: Implications for the extent of ice sheets and related proglacial lake systems. *Quaternary Science Reviews* 180, 240–259.  
<https://doi.org/10.1016/j.quascirev.2017.11.029>
- Laurat, T., Brühl, E., 2021. Neumark-Nord 2 – A multiphase Middle Palaeolithic open-air site in the Geisel Valley (Central Germany). *L’Anthropologie* 102936.  
<https://doi.org/10.1016/j.anthro.2021.102936>
- Laurat, T., Brühl, E., 2006. Zum Stand der archäologischen Untersuchungen im Tagebau Neumark-Nord, Ldkr. Merseburg- Querfurt (Sachsen-Anhalt) - Vorbericht zu den Ausgrabungen 2003-2005. *Jahresschrift für mitteldeutsche Vorgeschichte* 90, 9–69.
- Lisiecki, L.E., Raymo, M.E., 2005a. A Pliocene-Pleistocene stack of 57 globally distributed benthic  $\delta^{18}O$  records. *Paleoceanography* 20, 1–17.  
<https://doi.org/10.1029/2004PA001071>
- Lisiecki, L.E., Raymo, M.E., 2005b. A Pliocene-Pleistocene stack of 57 globally distributed benthic  $\delta^{18}O$  records. *Paleoceanography* 20, 1–17.  
<https://doi.org/10.1029/2004PA001071>
- Litt, T., Weber, T., 1988. Ein eemzeitlicher Waldelefantenschlachtplatz von Gröbern, Krs. Gräfenhainichen. *Ausgrabungen und Funde* 33, 181–187.
- Locht, J.-L., Hérisson, D., Goval, E., Cliquet, D., Huet, B., Coutard, S., Antoine, P., Fery, P., 2016. Timescales, space and culture during the Middle Palaeolithic in northwestern

- France. *Quaternary International* 411, 129–148.  
<https://doi.org/10.1016/j.quaint.2015.07.053>
- Machalett, B., Oches, E.A., Frechen, M., Zöller, L., Hambach, U., Mavlyanova, N.G., Marković, S.B., Endlicher, W., 2008. Aeolian dust dynamics in central Asia during the Pleistocene: Driven by the long-term migration, seasonality, and permanency of the Asiatic polar front. *Geochemistry, Geophysics, Geosystems* 9, n/a-n/a.  
<https://doi.org/10.1029/2007GC001938>
- Madella, M., Lancelotti, C., 2012. Taphonomy and phytoliths: A user manual. *Quaternary International* 275, 76–83. <https://doi.org/10.1016/j.quaint.2011.09.008>
- Mania, D., 2002. Der mittelpaläolithische Lagerplatz am Ascherslebener See bei Königsau (Nordharzvorland). *Præhistoria Thuringica* 8, 16–75.
- Mania, D., 1990. Auf den Spuren des Urmenschen: Die Funde aus der Steinrinne von Bilzingsleben. Deutscher Verlag der Wissenschaften, Berlin.
- Mania, D., Toepfer, V., 1973. Königsau: Gliederung, Ökologie und mittelpaläolithische Funde der letzten Eiszeit. Veröffentlichungen des Landesmuseums für Vorgeschichte in Halle 26, Deutscher Verlag der Wissenschaften, Berlin.
- Menke, B., 1976. Neue Ergebnisse zur Stratigraphie und Landschaftsentwicklung im Jungpleistozän Westholsteins. *E&G Quaternary Science Journal* 27, 53–68.  
<https://doi.org/10.3285/eg.27.1.05>
- Menke, B., Tynni, R., 1984. Das Eeminterglazial und das Weichselfrühglazial von Rederstell/Dithmarschen und ihre Bedeutung für die mitteleuropäische Jungpleistozän-Gliederung. *Geologisches Jahrbuch A* 76, 1–120.
- Meyer, K.D., 1983. Zur Anlage der Urstromtäler in Niedersachsen. *Z. Geomorph. N.F.* 27, 147–160.
- Mol, J., 1995. Weichselian and Holocene river dynamics in relation to climate change on the Halle-Leipziger Tieflandsbucht (Germany). *E & G Quaternary Science Journal* 45, 32–41.
- Moncel, M.-H., Neruda, P., 2000. The Kůlna level 11: Some observations on the debitage rules and aims. The originality of a Middle Palaeolithic microlithic assemblage (Kůlna Cave, Czech Republic). *Anthropologie XXXVIII*, 219–247.
- Moore, P.D., Webb, J.A., Collison, M.E., 1991. *Pollen analysis*. Blackwell Scientific Publications, Oxford.
- Moss, E., 1987. Polish G and the question of hafting, in: *La Main et l’outil: Manches et Emmanchements Préhistoriques*. G.S. Maison de l’Orient, pp. 97–102.
- Müller, U.C., Sánchez Goñi, Maria F., 2007. Vegetation dynamics in southern Germany during marine isotope stage 5 (~ 130 to 70 kyr ago), in: Sirocko, F., Claussen, M., Sánchez Goñi, M.F., Litt, T. (Eds.), *The Climate of Past Interglacials*. (Developments in Quaternary Sciences 7). pp. 277–287. [https://doi.org/10.1016/S1571-0866\(07\)80044-3](https://doi.org/10.1016/S1571-0866(07)80044-3)
- Murray, A.S., Wintle, A.G., 2003. The single aliquot regenerative dose protocol: potential for improvements in reliability. *Radiation Measurements* 37, 377–381.  
[https://doi.org/10.1016/S1350-4487\(03\)00053-2](https://doi.org/10.1016/S1350-4487(03)00053-2)
- NGRIP members, 2004. High-resolution record of Northern Hemisphere climate extending into the last interglacial period. *Nature* 431, 147–151. <https://doi:10.1038/nature02805>
- Nielsen, T.K., Benito, B.M., Svenning, J.-C., Sandel, B., McKerracher, L., Riede, F., Kjærgaard, P.C., 2017. Investigating Neanderthal dispersal above 55°N in Europe during the Last Interglacial Complex. *Quaternary International* 431, 88–103.  
<https://doi.org/10.1016/j.quaint.2015.10.039>
- Pastors, A., 2009. Blades ? – Thanks, no interest! - Neanderthals in Salzgitter-Lebenstedt. *Quartär* 56, 105–118.

- Pastors, A., 2001. Die Mittelpaläolithische Freilandstation von Salzgitter-Lebenstedt: Genese der Fundstelle und Systematik der Steinbearbeitung. Archiv der Stadt Salzgitter, Salzgitter.
- Pfaffenberg, K., 1991. Die Vegetationsverhältnisse während und nach der Sedimentation der Fundschichten von Salzgitter-Lebenstedt, in: Busch, R., Schwabedissen, H. (Eds.), *Der Altsteinzeitliche Fundplatz Salzgitter-Lebenstedt. Teil II. Naturwissenschaftliche Untersuchungen*. Böhlau Verlag, Köln, Weimar, Wien, pp. 183–210.
- Picin, A., 2016. Short-term occupations at the lakeshore: a technological reassessment of the open-air site Königsau (Germany). *Quartaer* 63, 7–32.  
[https://doi.org/10.7485/QU63\\_1](https://doi.org/10.7485/QU63_1)
- Pop, E., 2014. Analysis of the Neumark-Nord 2/2 lithic assemblage: results and interpretations, in: Gaudzinski-Windheuser, S., Roebroeks, W. (Eds.), *Multidisciplinary Studies of the Middle Palaeolithic Record from Neumark-Nord (Germany), Volume 1*. Veröffentlichungen des Landesamtes für Archäologie Sachsen-Anhalt - Landesmuseum für Vorgeschichte 69, Halle(Saale), pp. 143–195.
- Pop, E., Bakels, C., 2015. Semi-open environmental conditions during phases of hominin occupation at the Eemian Interglacial basin site Neumark-Nord 2 and its wider environment. *Quaternary Science Reviews* 117, 72–81.  
<https://doi.org/10.1016/j.quascirev.2015.03.020>
- Power, R.C., Rosen, A.M., Nadel, D., 2014. The economic and ritual utilization of plants at the Raqefet Cave Natufian site: The evidence from phytoliths. *Journal of Anthropological Archaeology* 33, 49–65. <https://doi.org/10.1016/j.jaa.2013.11.002>
- Preusser, F., 2004. Towards a chronology of the Late Pleistocene in the northern Alpine Foreland. *Boreas* 33, 195–210. <https://doi.org/10.1080/03009480410001271>
- Rae, T.C., Koppe, T., Stringer, C.B., 2011. The Neanderthal face is not cold adapted. *Journal of Human Evolution* 60, 234–239. <https://doi.org/10.1016/j.jhevol.2010.10.003>
- Rasmussen, S.O., Bigler, M., Blockley, S.P., Blunier, T., Buchardt, S.L., Clausen, H.B., Cvijanovic, I., Dahl-Jensen, D., Johnsen, S.J., Fischer, H., Gkinis, V., Guillevic, M., Hoek, W.Z., Lowe, J.J., Pedro, J.B., Popp, T., Seierstad, I.K., Steffensen, J.P., Svensson, A.M., Vallelonga, P., Vinther, B.M., Walker, M.J.C., Wheatley, J.J., Winstrup, M., 2014. A stratigraphic framework for abrupt climatic changes during the Last Glacial period based on three synchronized Greenland ice-core records: Refining and extending the INTIMATE event stratigraphy. *Quaternary Science Reviews* 106, 14–28.  
<https://doi.org/10.1016/j.quascirev.2014.09.007>
- Reuter, H.I., Nelson, A., Jarvis, A., 2007. An evaluation of void-filling interpolation methods for SRTM data. *International Journal of Geographical Information Science* 21, 983–1008.  
<https://doi.org/10.1080/13658810601169899>
- Richter, D., Krbetschek, M., 2014. Preliminary luminescence dating results for two Middle Palaeolithic occupations at Neumark-Nord 2, in: Gaudzinski-Windheuser, S., Roebroeks, W. (Eds.), *Multidisciplinary Studies of the Middle Palaeolithic Record from Neumark-Nord (Germany). Volume 1*. Veröffentlichungen des Landesamtes für Archäologie Sachsen-Anhalt - Landesmuseum für Vorgeschichte 69, Halle(Saale), pp. 131–136.
- Richter, J., 2016. Leave at the height of the party: A critical review of the Middle Paleolithic in Western Central Europe from its beginnings to its rapid decline. *Quaternary International* 411, 107–128. <https://doi.org/10.1016/j.quaint.2016.01.018>
- Richter, J., 2002. Die 14C-Daten aus der Sesselfelsgrötte und die Zeitstellung des Micoquien/MMO. *Germania* 80, 1–22.

- Richter, J., 1997. Sesselfelsgrötte III. Der G-Schichten-Komplex der Sesselfelsgrötte. Zum Verständnis des Micoquien, Quartär Bibliothek 7. Saarbrücker Druckerei und Verlag, Saarbrücken.
- Roebroeks, W., Bakels, C.C., Coward, F., Hosfield, R., Pope, M., Wenban-Smith, F., 2015. 'Forest Furniture' or 'Forest Managers'? On Neanderthal presence in Last Interglacial environments, in: *Settlement, Society and Cognition in Human Evolution*. Cambridge University Press, New York, pp. 174–188.  
<https://doi.org/10.1017/CBO9781139208697.011>
- Roebroeks, W., Hublin, J.-J., MacDonald, K., 2011. Continuities and Discontinuities in Neanderthal Presence: A Closer Look at Northwestern Europe, in: *Developments in Quaternary Sciences*. Elsevier, pp. 113–123. <https://doi.org/10.1016/B978-0-444-53597-9.00008-X>
- Rots, V., 2010. Prehension and hafting traces on flint tools: a methodology. Universitaire Press Leuven.
- Schwan, J., 1988. The structure and genesis of Weichselian to early holoene aeolian sand sheets in western Europe. *Sedimentary Geology* 55, 197–232.  
[https://doi.org/10.1016/0037-0738\(88\)90132-7](https://doi.org/10.1016/0037-0738(88)90132-7)
- Selle, W., 1991. Die palynologischen Untersuchungen am paläolithischen Fundplatz Salzgitter-Lebenstedt, in: Busch, R., Schwabedissen, H. (Eds.), *Der Altsteinzeitliche Fundplatz Salzgitter-Lebenstedt. Teil II. Naturwissenschaftliche Untersuchungen*. Böhlau Verlag, Köln, Weimar, Wien, pp. 149–161.
- Semenov, S.A., 1964. *Prehistoric Technology: an Experimental Study of the Oldest Tools and Artifacts from Traces of Manufacture and Wear*. Barnes and Noble.
- Skrzypek, G., Wiśniewski, A., Grierson, P.F., 2011. How cold was it for Neanderthals moving to Central Europe during warm phases of the last glaciation? *Quaternary Science Reviews* 30, 481–487.
- Stephan, H.-J., 2014. Climato-stratigraphic subdivision of the Pleistocene in Schleswig-Holstein, Germany and adjoining areas: status and problems. *E&G Quaternary Science Journal* 63, 3–18. <https://doi.org/10.3285/eg.63.1.01>
- Stephan, H.-J., Burbaum, B., Kenzler, M., Krienke, K., Lungershausen, U., Tummuscheit, A., Frechen, M., Thiel, C., Urban, B., Sierralta, M., 2017. Quartärgeologie und Archäologie im Norden Schleswig-Holsteins (unpublished field trip guide).
- Stoops, G., 2003. *Guidelines for Analysis and Description of Soil and Regolith Thin Sections*. Soil Science Society of America, Inc, Madison, Wisconsin, USA.
- Stoops, G., Marcelino, V., Mees, F., 2010. Interpretation of Micromorphological Features of Soils and Regoliths, *Interpretation of Micromorphological Features of Soils and Regoliths*. <https://doi.org/10.1016/C2009-0-18081-9>
- Strahl, J., Krbetschek, M.R., Luckert, J., Machalet, B., Meng, S., Ochse, E.A., Rappsilber, I., Wansa, S., Zöller, L., 2010. Geologie, Paläontologie und Geochronologie des Eem-Beckens Neumark-Nord 2 und Vergleich mit dem Becken Neumark-Nord 1 (Geiseltal, Sachsen-Anhalt). *Eiszeitalter und Gegenwart (Quaternary Science Journal)* 59, 120–167.  
<https://doi.org/10.3285/eg.59.1-2.09>
- Taylor, G.H., Teichmüller, M., Davis, A., Diessel, C.F.K., Littke, R., Robert, P., 1998. *Organic Petrology*. Gebrüder Bornträger, Berlin Stuttgart.
- Thiel, C., Buylaert, J.P., Murray, A., Terhorst, B., Hofer, I., Tsukamoto, S., Frechen, M., 2011. Luminescence dating of the Stratzing loess profile (Austria) - Testing the potential of an elevated temperature post-IR IRSL protocol. *Quaternary International* 234, 23–31.  
<https://doi.org/10.1016/j.quaint.2010.05.018>

- Thieme, H., 2003. Ochtmissen, Stadt Lüneburg – ein faustkeilreicher Fundplatz des späten Acheuléen in der Ilmenau- Niederung., in: Burdukiewicz, J.M., Justus, A., L., F. (Eds.), Erkenntnisjäger. Kultur Und Umwelt Des Frühen Menschen. Festschrift Für Dietrich Mania, Veröffentlichungen Des Landesamtes Für Denkmalpflege Und Archäologie Sachsen-Anhalt, Landesmuseum Für Vorgeschichte 57. Veröffentlichungen des Landesamtes für Denkmalpflege und Archäologie Sachsen-Anhalt, Landesmuseum für Vorgeschichte, Bd. 57, Halle(Saale), pp. 593–600.
- Thieme, H., Veil, S., 1985. Neue Untersuchungen zum eemzeitlichen Elefanten-Jagdplatz Lehringen, Ldkr. Verden. Die Kunde N.F. 36, 11–58.
- Tode, A., 1982. Der altsteinzeitliche Fundplatz Salzgitter-Lebenstedt. Teil I, archäologischer Teil. Böhlau, Köln, Wien.
- Toepfer, V., 1958. Steingeräte und Palökologie der mittel- paläolithischen Fundstelle Rabutz bei Halle. Jahresschrift für mitteldeutsche Vorgeschichte 41/42, 140–179.
- Tucci, M., Krahn, K.J., Richter, D., van Kolfshoten, T., Álvarez, B.R., Verheijen, I., Serangeli, J., Lehmann, J., Degering, D., Schwalb, A., Urban, B., 2021. Evidence for the age and timing of environmental change associated with a Lower Palaeolithic site within the Middle Pleistocene Reinsdorf sequence of the Schöningen coal mine, Germany. *Palaeogeography, Palaeoclimatology, Palaeoecology* 569, 110309. <https://doi.org/10.1016/j.palaeo.2021.110309>
- Valoch, K., 1988. Die Erforschung der Kůlna Höhle 1961–1976. Moravské Muzeum, Brno.
- Van Huissteden, K., Vandenberghe, J., Pollard, D., 2003. Palaeotemperature reconstructions of the European permafrost zone during marine oxygen isotope Stage 3 compared with climate model results. *Journal of Quaternary Science* 18, 453–464. <https://doi.org/10.1002/jqs.766>
- Van Meerbeeck, C.J., Renssen, H., Roche, D.M., Wohlfarth, B., Bohncke, S.J.P., Bos, J.A.A., Engels, S., Helmens, K.F., Sánchez-Goñi, M.F., Svensson, A., Vandenberghe, J., 2011. The nature of MIS 3 stadial–interstadial transitions in Europe: New insights from model–data comparisons. *Quaternary Science Reviews* 30, 3618–3637. <https://doi.org/10.1016/j.quascirev.2011.08.002>
- Vandenberghe, J., 2013. Cryoturbation Structures, in: S.A, E. (Ed.), *The Encyclopedia of Quaternary Science*, pp. 430–435.
- Vandenberghe, J., Pissart, A., 1993. Permafrost changes in Europe during the last glacial. *Permafrost and Periglacial Processes* 4, 121–135. <https://doi.org/10.1002/ppp.3430040205>
- Vandenberghe, J., Van den Broek, P., 1982. Weichselian Convolution Phenomena and processes in fine sediments. *Boreas* 11, 299–315. <https://doi.org/10.1111/j.1502-3885.1982.tb00539.x>
- Vandenberghe, J., van der Plicht, J., 2016. The age of the Hengelo interstadial revisited. *Quaternary Geochronology* 32, 21–28. <https://doi.org/10.1016/j.quageo.2015.12.004>
- Vaughan, P.C., 1985. Use-wear analysis of flaked stone tools. University of Arizona Press Tucson.
- Veil, S., 1995. Vor 55.000 Jahren. Ein Jagdplatz früher Menschen bei Lichtenberg, Ldkr Lüchow-Dannenberg, Begleithefte zu Ausstellungen der Abteilung Urgeschichte des Niedersächsischen Landesmuseums Hannover; H.5. Isensee Verlag, Oldenburg.
- Veil, S., Breest, K., Höfle, H.-C., Meyer, H.-H., Plisson, H., Urban-Küttel, B., Wagner, G.A., Zöller, L., 1994. Ein mittelpaläolithischer Fundplatz aus der Weichsel-Kaltzeit bei Lichtenberg, Lkr. Lüchow-Dannenberg. *Germania* 72, 1–66.

- Walkling, A., 1997. Käferkundliche Untersuchungen an weichselzeitlichen Ablagerungen der Bohrung Groß Todtshorn (Kr. Harburg; Niedersachsen). *Schriftenreihe der Deutschen Geologischen Gesellschaft* 4, 87–102.
- Weber, T., 1990. Paläolithische Funde aus den Eemvorkommen von Rabutz, Grabschütz und Gröbern, in: Eißmann, L. (Ed.), *Die Eemwarmzeit Und Die Frühe Weichsel- Eiszeit Im Saale-Elbe-Gebiet. Geologie, Paläontologie, Palökologie, Altenburger Naturwissenschaftliche Forschungen 5. Naturkundliches Museum Mauritianum, Altenburg.*
- Weiss, M., 2020. The Lichtenberg Keilmesser - it's all about the angle. *PLOS ONE* 15, e0239718. <https://doi.org/10.1371/journal.pone.0239718>
- Weiss, M., 2019. Beyond the caves: stone artifact analysis of late Middle Paleolithic open-air assemblages from the European Plain. PhD Thesis, Universiteit Leiden.
- Weiss, M., 2015. Stone tool analysis and context of a new late Middle Paleolithic site in western central Europe - Pouch-Terrassenpfeiler, Ldkr. Anhalt-Bitterfeld, Germany. *Quartär* 62, 23–62. [https://doi.org/10.7485/QU62\\_2](https://doi.org/10.7485/QU62_2)
- Weiss, M., Lauer, T., Wimmer, R., Pop, C.M., 2018. The Variability of the Keilmesser-Concept: a Case Study from Central Germany. *Journal of Paleolithic Archaeology* 1, 202–246. <https://doi.org/10.1007/s41982-018-0013-y>
- Weißmüller, W., 1995. Die Silexartefakte der Unteren Schichten der Sesselfelsgrötte. Ein Beitrag zum Problem des Moustérien, *Quartärbibliothek* 6. Saarbrücker Druckerei und Verlag, Saarbrücken.
- White, M.J., Pettitt, P.B., 2011. The British Late Middle Palaeolithic: An Interpretative Synthesis of Neanderthal Occupation at the Northwestern Edge of the Pleistocene World. *Journal of World Prehistory* 24, 25–97. <https://doi.org/10.1007/s10963-011-9043-9>
- Winsemann, J., Lang, J., Roskosch, J., Polom, U., Böhner, U., Brandes, C., Glotzbach, C., Frechen, M., 2015. Terrace styles and timing of terrace formation in the Weser and Leine valleys, northern Germany: Response of a fluvial system to climate change and glaciation. *Quaternary Science Reviews* 123, 31–57. <https://doi.org/10.1016/j.quascirev.2015.06.005>
- Wintle, A.G., Adamiec, G., 2017. Optically stimulated luminescence signals from quartz: A review. *Radiation Measurements* 98, 10–33. <https://doi.org/10.1016/j.radmeas.2017.02.003>
- Wiśniewski, A., Chłoń, M., Weiss, M., Pyżewicz, K., Migal, W., 2020. On Making of Micoquian Bifacial Backed Tools at Pietraszyn 49a, SW Poland. *Journal of Paleolithic Archaeology*. <https://doi.org/10.1007/s41982-020-00069-y>
- Wiśniewski, A., Lauer, T., Chłoń, M., Pyżewicz, K., Weiss, M., Badura, J., Kalicki, T., Zarzecka-Szubińska, K., 2019. Looking for provisioning places of shaped tools of the late Neanderthals: A study of a Micoquian open-air site, Pietraszyn 49a (southwestern Poland). *Comptes Rendus Palevol* 18, 367–389. <https://doi.org/10.1016/j.crpv.2019.01.003>
- Wiśniewski, A., Adamiec, G., Badura, J., Bluszcz, A., Kowalska, A., Kufel-Diakowska, B., Mikołajczyk, A., Murczkiewicz, M., Musil, R., Przybylski, B., Skrzypek, G., Stefaniak, K., Zych, J., 2013. Occupation dynamics north of the Carpathians and Sudetes during the Weichselian (MIS5d-3): The Lower Silesia (SW Poland) case study. *Quaternary International* 294, 20–40. <https://doi.org/10.1016/j.quaint.2011.09.016>
- Woillard, G., 1979. The last interglacial-glacial cycle at Grande Pile in Northeastern France. *Bulletin Société belge de Géologie* 88, 51–69.

Zagwijn, W., Paepe, R., 1968. Die Stratigraphie der weichselzeitlichen Ablagerungen der Niederlande und Belgiens. *E&G – Quaternary Science Journal* 19, 10–31.

### **Author Contributions**

All authors made substantial contributions to the study and approved the final manuscript. M.H. and M.W. equally contributed to the study with respect to research design, fieldwork, data analyses, interpretation of data and the writing of the manuscript. They actively took part in the different analyses listed below and amalgamated the various data. B.U. and M.T. conducted palynological analysis; M.C.S. and S.H. conducted micromorphological analysis; Y.H.H. performed traceology on the artefacts; R.C.P. did phytolith analysis; H. v.S. co-supervised M.H. s doctoral thesis and supported fieldwork; T.T., U.B., F.K. provided additional archaeological data of the region and supported fieldwork; S.V. and K.B. discovered and excavated the original site; J.S. supported grain size analysis; D.C. supported luminescence dating; D.C.T. and M.F. provided methodological and geological information; T.L. supervised M.H. s doctoral thesis, contributed to the research design and supported luminescence dating. All authors contributed to the preparation of the manuscript.